Sparse Cholesky factorization by greedy conditional selection

Stephen Huan[*], Joe Guinness[†], Matthias Katzfuss[‡], Houman Owhadi[§], and Florian Schäfer[¶]

Abstract. Dense kernel matrices resulting from pairwise evaluations of a kernel function arise naturally in machine learning and statistics. Previous work in constructing sparse transport maps or sparse approximate inverse Cholesky factors of such matrices by minimizing Kullback-Leibler divergence recovers the Vecchia approximation for Gaussian processes. These methods rely only on the geometry of the evaluation points to construct the sparsity pattern. In this work, we instead construct the sparsity pattern by leveraging a greedy selection algorithm that maximizes mutual information with target points, conditional on all points previously selected. For selecting k points out of N, the naive time complexity is $\mathcal{O}(Nk^4)$, but by maintaining a partial Cholesky factor we reduce this to $\mathcal{O}(Nk^2)$. Furthermore, for multiple (m) targets we achieve a time complexity of $\mathcal{O}(Nk^2 + Nm^2 + m^3)$ which is maintained in the setting of aggregated Cholesky factorization where a selected point need not condition every target. We apply the selection algorithm to image classification and recovery of sparse Cholesky factors. By minimizing Kullback-Leibler divergence, we apply the algorithm to Cholesky factorization, Gaussian process regression, and preconditioning with the conjugate gradient, improving over k-nearest neighbors particularly in high dimensional, unusual, or otherwise messy geometries.

Key words. to do

AMS subject classifications.

1. Introduction.

The problem. Gaussian processes are widely used in spatial statistics and geostatistics [45], machine learning through kernel methods [44], optimal experimental design [39], and sensor placement [34]. Applying Gaussian process statistics to sets of N data points requires computing with the covariance matrix $\Theta \in \mathbb{R}^{N \times N}$ to obtain quantities such as $\Theta \boldsymbol{v}$, $\Theta^{-1} \boldsymbol{v}$, $\mathrm{logdet}(\Theta)$. For dense Θ, directly computing these quantities has a computational cost of $\mathcal{O}(N^3)$ and a memory cost of $\mathcal{O}(N^2)$, which is prohibitively expensive for large N. Beyond Gaussian processes, computations with large positive-definite matrices are required across computational mathematics, motivating the search for faster, approximate algorithms.

Existing work. Numerous methods have been proposed for fast approximate Gaussian process statistics. Popular methods are based on low-rank approximation [51, 65, 16, 3, 17, 11], sparse approximations [18], or combinations thereof [49, 42, 4, 46]. These approximations can be viewed as imposing different (conditional) independence structures on the Gaussian process. Multiscale-versions of these ideas lead to wavelets [7, 19] and various structured matrix factorizations [25, 24, 9, 66, 36, 1, 2, 28, 48]. Alternatives are based on fast Fourier transforms [20, 53] or random feature maps [43].

[*]Georgia Institute of Technology
[†]Joe
[‡]Matthias
[§]Houman
[¶]Georgia Institute of Technology, S1317 CODA, 756 W Peachtree St Atlanta, GA 30332, florian.schaefer@cc.gatech.edu, Corresponding Author

Vecchia approximation, Kaporin's factorization, and KL minimization. Vecchia approximates the likelihood function of a Gaussian distribution by decomposing it into a product of univariate conditional densities, each of which depends on a subset of the previous variables [61]. Independently from Vecchia, Kaporin derived a closed-form expression of the approximate inverse Cholesky preconditioner of a p.s.d. matrix that minimizes, subject to a sparsity constraint, the K-condition number of the preconditioned system [31]. Referring to this approximation as "factorized sparse approximate inverse (FSAI)," Yeremin et al. show that Kaporin's inverse Cholesky factor also minimizes a Frobenius-norm error metric, subject to a diagonal scaling constraint [67]. Vecchia's likelihood approximation was later observed to implicitly compute a sparse approximate inverse Cholesky factor of the covariance matrix [32]. The closed-form expression of this inverse Cholesky factor coincides with that derived by Kaporin. Independently from the above works, Schäfer et al. compute sparse inverse Cholesky factors that are optimal in Kullback-Leibler (KL) divergence [47], again recovering the formula derived by Kaporin. The KL divergence is also used to compute Knothe-Rosenblatt transport maps [38], generalizing Cholesky factors to non-Gaussian distributions while preserving triangularity and sparsity [52]. A method for the Bayesian estimation of such transport maps is proposed by [33]. A common feature of the above methods is that the columns of the Cholesky factors can be computed independently and in parallel.

Ordering and sparsity selection by geometry. The approximation quality of the above methods depends on the ordering of the rows and columns of the input matrix and the sparsity pattern of the factor. Vecchia originally proposed ordering points lexicographically [61]. The work on FSAI emphasized classical orderings from sparse linear algebra such as (reverse) Cuthill-McKee, minimum degree, nested dissection, and red-black ordering [6]. Guinness empirically studied the effect of various orderings on Vecchia's likelihood approximation [23]. He found the random ordering and a space-filling maximum-minimum distance (maximin) ordering to perform well. This observation can be explained by the *screening effect*, by which conditional on points near the point of interest, far away points are almost conditionally independent for many popular kernel functions [54, 55] (see Figure 1). Cholesky factorization is closely related to numerical homogenization and operator adapted wavelets [40]. Schäfer et al. exploit this connection to prove exponential decay of Cholesky factors of covariance and precision matrices arising from elliptic PDEs, when developed in a multiresolution basis [48]. This setting includes the maximin ordering as a simplistic multiresolution basis akin to the "lazy wavelet" [58] and thus provides a rigorous proof of the screening effect. The maximin ordering has since been used by [47, 32, 30, 33]. Motivated by the screening effect, the sparsity set is often formed by selecting the closest points by Euclidean distance [61, 48, 47, 33]. To lower the computational cost, different authors have proposed heuristics to analyze the sparsity set and identify opportunities to group similar degrees of freedom into supernodes [56, 15, 23]. Schäfer et al. devise a geometric grouping algorithm that allows to provably compute an ϵ-accurate inverse-Cholesky factor in time complexity $\mathcal{O}(N \log^{2d}(N/\epsilon))$ using $\mathcal{O}(N \log^{d}(N/\epsilon))$ nonzero entries of the covariance matrix [47]. Methods based on the screening effect have improved the state-of-the-art for solving elliptic differential and integral equations [48, 47, 10]. However, selecting the sparsity set only based on distance ignores the possible redundancy of the selected points. The proposed work addresses this limitation.
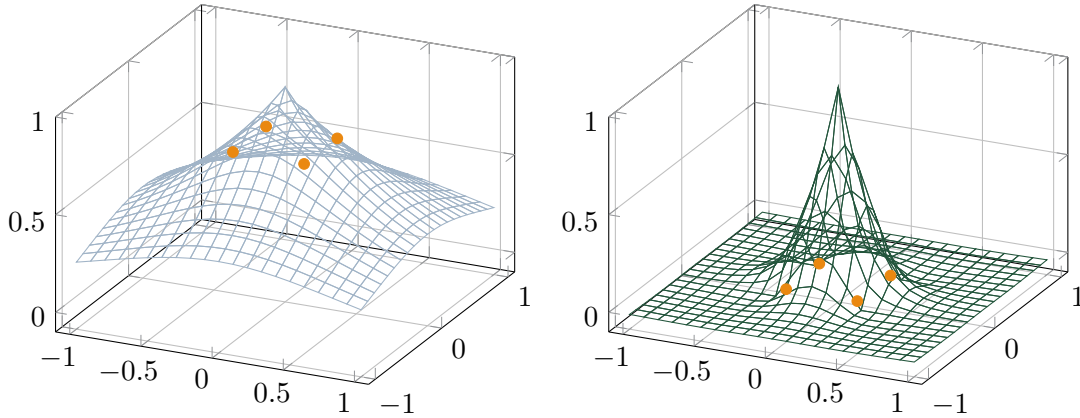
Figure 1. *An illustration of the screening effect with the Matérn kernel with length scale $\ell = 1$ and smoothness $\nu = 1/2$. The first panel shows the* unconditional correlation *with the point at (0, 0). The second panel shows the* conditional correlation *after conditioning on the four points in* orange.

Conditional selection. Instead of adding points to the sparsity pattern by distance, we propose greedily selecting points that maximize mutual information with the point of interest, conditional on all points previously selected. The machine learning community has long developed similar algorithms that greedily optimize information-theoretic objectives in the context of sparse Gaussian process inference [51, 27, 50]. Similar algorithms have also been developed in the context of sensor placement [34, 12] and experimental design [39] where it is assumed the target phenomenon is modeled by a Gaussian process or is otherwise linearly dependent on the selected measurements. However, these works often focus on global approximation of the entire process, e.g., through sparse approximation of the likelihood or covariance matrix [37, 8, 42]. In contrast [64] uses inference *directed* towards a point of interest, selecting the active (sparsity) set by the kernel function itself like the later work [30]; [21] and the follow-up work [22] use the more sophisticated active learning Cohn (ALC) objective, yielding an algorithm equivalent to ours for a single point of interest. Our proposed algorithm can also be viewed as a variant of orthogonal matching pursuit (OMP) [59, 60], a workhorse algorithm in compressive sensing, which seeks to approximate a target signal as the sparse linear combination from a given collection of signals.

Main results. Our main contribution is a selection algorithm that greedily maximizes mutual information with point(s) of interest, conditional on all points previously selected. We use this algorithm to select the sparsity pattern of sparse approximate Cholesky factors of precision matrices in the KL-minimization framework of [47], improving the approximation accuracy attainable with a given number of nonzero entries. Our method extends kernel-based selection [64, 30] to account for conditioning. It also extends directed Gaussian process regression [21, 22] by simultaneously targeting multiple prediction points and providing a global approximation of the Gaussian process. For a single target point, naive computation of the mutual information criterion has time complexity $\mathcal{O}(Nk^4)$ to select k points out of N. By maintaining a partial Cholesky factor we reduce the complexity to $\mathcal{O}(Nk^2)$. We extend the algorithm to maximize mutual information with *multiple* targets, re-using the same selections
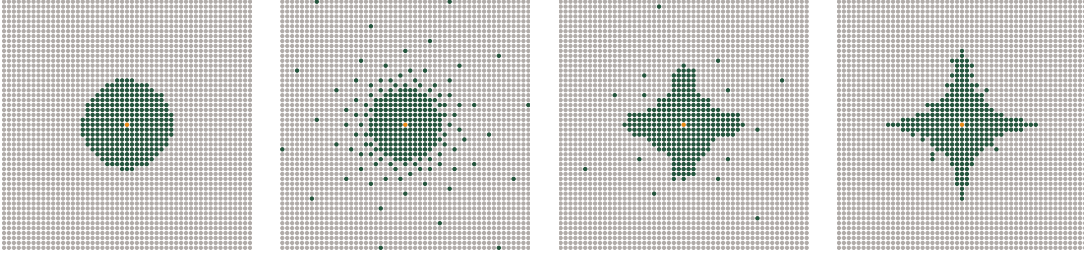
Figure 2. *The first panel shows selecting the k-nearest neighbors to the center point out of a dense grid of candidates. The next panels show selection by greedily maximizing conditional mutual information with the center point for a Matérn kernel with length scale $\ell = 1$ and increasing smoothness ν, from right to left: $\nu = 1/2, 3/2, 5/2$. The full selections are found at https://youtu.be/lyJf3S5ThjQ.*

across multiple targets for efficiency while maintaining accuracy. For m target points we achieve a time complexity of $\mathcal{O}(Nk^2 + Nm^2 + m^3)$. If $m \approx k$, this is m times faster than the single-target algorithm. In the setting of aggregated (or supernodal) Cholesky factorization where the sparsity patterns of multiple columns are determined simultaneously, a candidate entry may only condition a *subset* of the targets. By efficient rank-one downdating of Cholesky factors, we capture this structure at the same time complexity for multiple targets. Finally, we show how to adaptively determine the number of nonzeros per column in order to minimize the overall KL divergence by maintaining a global priority queue shared between all columns.

Outline. This paper is organized as follows. In section 2, we show how minimizing KL divergence to compute sparse Cholesky factors reduces to solving independent regression problems. In section 3, we develop greedy algorithms to select the sparsity pattern independently for each regression problem. In section 4, we combine the greedy selection algorithm with KL minimization to yield algorithms for sparse Cholesky factorization. In section 5 we extend these results to adjacent and nonadjacent aggregated factorization. In section 6, we present numerical experiments applying our method to Cholesky factorization, Gaussian process regression, preconditioning with the conjugate gradient, image classification, and recovery of *a priori* sparse Cholesky factors. In section 7, we summarize our results. Proofs and algorithmic details are provided in the appendix and supplementary material.

2. Sparse Cholesky factorization by KL-minimization. Let $\Theta \in \mathbb{R}^{N \times N}$ be a symmetric positive-definite matrix; we view Θ as the covariance matrix of a Gaussian process. We say that a function $f(\boldsymbol{x})$ is distributed according to a Gaussian process prior with mean function $\mu(\boldsymbol{x})$ and covariance function or kernel function $K(\boldsymbol{x}, \boldsymbol{x}')$, which we will denote as $f(\boldsymbol{x}) \sim \mathcal{GP}(\mu(\boldsymbol{x}), K(\boldsymbol{x}, \boldsymbol{x}'))$, if for any finite set of points $X = \{\boldsymbol{x}_i\}_{i=1}^N$, $f(X) \sim \mathcal{N}(\boldsymbol{\mu}, \Theta)$, where $\mu_i = \mu(\boldsymbol{x}_i)$ and $\Theta_{i,j} = K(\boldsymbol{x}_i, \boldsymbol{x}_j)$.

In many applications of Gaussian processes, we wish to infer unknown data given known data. Given the training dataset $\mathcal{D} = \{(\boldsymbol{x}_i, y_i)\}_{i=1}^N$ where the inputs $\boldsymbol{x}_i \in \mathbb{R}^D$ are collected in the matrix $X_{\text{Tr}} = [\boldsymbol{x}_1, \dots, \boldsymbol{x}_N]^\top \in \mathbb{R}^{N \times D}$ and the measurements at those points are collected in the vector $\boldsymbol{y}_{\text{Tr}} = [y_1, \dots, y_N]^\top \in \mathbb{R}^N$, we wish to predict the values at m new points $X_{\text{Pr}} \in \mathbb{R}^{m \times D}$ for which $\boldsymbol{y}_{\text{Pr}} \in \mathbb{R}^m$ is unknown. We assume the function $f(\boldsymbol{x})$ that maps input points to their outputs is distributed according to a Gaussian process with zero mean function,

137 $f(\boldsymbol{x}) \sim \mathcal{GP}(\boldsymbol{0}, K(\boldsymbol{x}, \boldsymbol{x}'))$. From the distribution of $f(\boldsymbol{x})$, the joint distribution of training and

138 testing data $\boldsymbol{y}$ has covariance $\Theta = \begin{pmatrix} \Theta_{\mathrm{Tr},\mathrm{Tr}} & \Theta_{\mathrm{Tr},\mathrm{Pr}} \\ \Theta_{\mathrm{Pr},\mathrm{Tr}} & \Theta_{\mathrm{Pr},\mathrm{Pr}} \end{pmatrix}$ where $\Theta_{I,J} := K(X_I, X_J)$ for index sets

139 I, J. In order to make predictions at X_{Pr}, we condition the desired prediction $\boldsymbol{y}_{\mathrm{Pr}}$ on the

140 known data $\boldsymbol{y}_{\mathrm{Tr}}$. For Gaussian processes, the closed-form posterior distribution is

141 (2.1) $$\mathbb{E}[\boldsymbol{y}_{\mathrm{Pr}} \mid \boldsymbol{y}_{\mathrm{Tr}}] = \boldsymbol{\mu}_{\mathrm{Pr}} + \Theta_{\mathrm{Pr},\mathrm{Tr}} \Theta_{\mathrm{Tr},\mathrm{Tr}}^{-1} (\boldsymbol{y}_{\mathrm{Tr}} - \boldsymbol{\mu}_{\mathrm{Tr}})$$

142 (2.2) $$\mathbb{C}\mathrm{ov}[\boldsymbol{y}_{\mathrm{Pr}} \mid \boldsymbol{y}_{\mathrm{Tr}}] = \Theta_{\mathrm{Pr},\mathrm{Pr}} - \Theta_{\mathrm{Pr},\mathrm{Tr}} \Theta_{\mathrm{Tr},\mathrm{Tr}}^{-1} \Theta_{\mathrm{Tr},\mathrm{Pr}}$$

where $\Theta_{\mathrm{Tr},\mathrm{Tr}}^{-1} := (\Theta_{\mathrm{Tr},\mathrm{Tr}})^{-1}$. To denote the covariance between the variables in index sets I

143 and J, conditional on the variables in the index sets $V_1, V_2, \ldots, V_n$ we write

144 (2.3) $$\Theta_{I,J|V_1,V_2,\ldots,V_n} := \mathbb{C}\mathrm{ov}[\boldsymbol{y}_I, \boldsymbol{y}_J \mid \boldsymbol{y}_{V_1 \cup V_2 \cup \cdots \cup V_n}].$$

145 We recursively compute (2.3); let $W = \bigcup_{i=1}^{n-1} V_i$ and by the quotient rule of Schur complements,

146 (2.4) $$\Theta_{I,J|V_1,\ldots,V_n} = \Theta_{I,J|W} - \Theta_{I,V_n|W} \Theta_{V_n,V_n|W}^{-1} \Theta_{V_n,J|W}.$$

147   Calculating the posterior mean (2.1) and covariance (2.2) requires inverting the training
148 covariance matrix, usually by means of Cholesky factorization. The time complexity of com-
149 puting the Cholesky factorization is $\mathcal{O}(N^3)$, which is prohibitive for large N. Thus, we aim
150 to compute *sparse* approximate Cholesky factors.

151   **2.1. Vecchia approximation.** The Vecchia approximation for Gaussian processes [61] can
152 be viewed as computing sparse approximate inverse-Cholesky factors of Θ. It decomposes the
153 joint likelihood π as

154 (2.5) $$\pi(\boldsymbol{y}) = \pi(y_1) \, \pi(y_2 \mid y_1) \, \pi(y_3 \mid y_1, y_2) \cdots \pi(y_N \mid y_1, y_2, \ldots, y_{N-1}).$$

The key assumption is that many of the conditioning points are redundant. Letting $i_1, \ldots, i_N$
denote an ordering of the points and s_k the indices of points that condition the kth point in
155 the ordering, the Vecchia approximation proposes replacing (2.5) by the sparse approximation

156 (2.6) $$\pi(\boldsymbol{y}) \approx \pi(y_{i_1}) \, \pi(y_{i_2} \mid y_{s_2}) \, \pi(y_{i_3} \mid y_{s_3}) \cdots \pi(y_{i_N} \mid y_{s_N}).$$

157 The precision matrix of the resulting approximate density (2.6) has a sparse Cholesky factor
158 in the sense that the ith column of the factor has the sparsity pattern s_i when written in
159 the given elimination ordering [32]. Another way to recover this Cholesky factor for a fixed
160 elimination ordering $\prec$ and lower triangular sparsity pattern $S := \{(i,j) : i \in s_j, i \succeq j\}$ is to
161 specify a functional criterion $\mathcal{L} : \mathbb{R}^{N \times N} \to \mathbb{R}$ defining an optimization problem over candidate
162 matrices satisfying the sparsity pattern, $\mathcal{S} := \{M \in \mathbb{R}^{N \times N} : M_{i,j} \neq 0 \Rightarrow (i,j) \in S\}$.

163 (2.7) $$L := \underset{\hat{L} \in \mathcal{S}}{\mathrm{argmin}} \, \mathcal{L}(\hat{L})$$

164 Functionals include the Kaporin condition number $(\mathrm{trace}(L\Theta L^\top)/N)^N / \det(L\Theta L^\top)$ [31], the
165 Frobenius norm $\|\mathrm{Id} - L\,\mathrm{chol}(\Theta)\|_{\mathrm{FRO}}$ additionally subject to the constraint $\mathrm{diag}(L\Theta L^\top) = 1$
166 [67], and the Kullback-Leiber (KL) divergence $\mathbb{D}_{\mathrm{KL}}(\mathcal{N}(\boldsymbol{0}, \Theta) \parallel \mathcal{N}(\boldsymbol{0}, (LL^\top)^{-1}))$ [47]. These
167 three choices all recover the Vecchia approximation.

As observed in [45, 47], factors of the precision matrix are often much sparser than factors of the covariance matrix, because the precision encodes conditional independence while the covariance encodes marginal independence. The same phenomenon is observed by [52] working with the more general transport maps. Covariance matrices arising from kernel functions are often fully dense, but the approximate factors of their precisions can be sparse if their ordering and sparsity pattern are chosen carefully.

2.2. Ordering and sparsity pattern. Although in this work we primarily focus on constructing sparsity patterns, the chosen ordering critically affects the accuracy of lower triangular sparsity patterns. Vecchia originally proposed ordering points lexicographically, which is most natural in a one-dimensional setting [61]. More recent work finds that in higher dimensions, exploiting space-covering orderings leads to significantly better approximation quality [23]. Specifically, we use the maximum-minimum (maximin) ordering [23], which has become popular for the Vecchia approximation [32] and Cholesky factorization [48, 47, 30, 33]. The reverse-maximin ordering $i_1, \ldots, i_N$ on a set of N points $\{\boldsymbol{x}_i\}_{i=1}^N$ is defined by first selecting the last index i_N arbitrarily and then choosing for $k = N - 1, N - 2, \ldots, 1$ the index

$$(2.8) \qquad i_k = \operatorname*{argmax}_{i \in -\mathcal{I}_{k+1}} \min_{j \in \mathcal{I}_{k+1}} \|\boldsymbol{x}_i - \boldsymbol{x}_j\|$$

where $-\mathcal{I} := \{1, \ldots, N\} \setminus \mathcal{I}$ and $\mathcal{I}_n := \{i_n, i_{n+1}, \ldots, i_N\}$, i.e. select the point farthest from previously selected points. The ordering is reversed for factorizing the precision. We write $i \prec j$ if i precedes j in the ordering and define $\ell_{i_k} := \min_{j \in \mathcal{I}_{k+1}} \|\boldsymbol{x}_{i_k} - \boldsymbol{x}_j\|$, a length scale monotonically shrinking with decreasing position in the ordering.

Vecchia also originally proposed to select the sparsity set by Euclidean distance [61], which, unlike the lexicographic ordering, still remains widely used [48, 47, 33]. Instead, we will select the sparsity pattern to directly optimize the accuracy $\mathcal{L}$ (2.7).

2.3. Review of KL-minimization. The Kullback-Leibler (KL) divergence between two probability distributions P and Q is defined as $\mathbb{D}_{\mathrm{KL}}(P \parallel Q) := \mathbb{E}_P[\log(\frac{P}{Q})]$. As the expected difference between true and approximate log-densities, the KL divergence naturally judges the quality of an approximating distribution. We identify the positive-definite matrix $\Theta \in \mathbb{R}^{N \times N}$ as the covariance matrix of a centered Gaussian process $\mathcal{N}(\boldsymbol{0}, \Theta)$ which we seek to approximate by a sparse approximate Cholesky factor $L \in \mathcal{S}$ of its precision, $\mathcal{N}(\boldsymbol{0}, (LL^\top)^{-1})$. We compare these distributions by the KL divergence as [47] does, specializing the generic optimization problem (2.7) to

$$(2.9) \qquad L := \operatorname*{argmin}_{\hat{L} \in \mathcal{S}} \mathbb{D}_{\mathrm{KL}}\left(\mathcal{N}(\boldsymbol{0}, \Theta) \,\middle\|\, \mathcal{N}(\boldsymbol{0}, (\hat{L}\hat{L}^\top)^{-1})\right).$$

For multivariate Gaussians, the KL divergence has a closed-form expression given by

$$(2.10) \qquad 2\mathbb{D}_{\mathrm{KL}}(\mathcal{N}(\boldsymbol{0}, \Theta_1) \parallel \mathcal{N}(\boldsymbol{0}, \Theta_2)) = \operatorname{trace}(\Theta_2^{-1}\Theta_1) + \operatorname{logdet}(\Theta_2) - \operatorname{logdet}(\Theta_1) - N$$

where $\Theta_1, \Theta_2 \in \mathbb{R}^{N \times N}$. Using this expression for the KL divergence and optimizing for L yields the following closed-form expression for the nonzero entries in the ith column of L with

204 sparsity pattern s_i, reproduced from Theorem 2.1 of [47]:

205 (2.11)
$$L_{s_i,i} = \frac{\Theta_{s_i,s_i}^{-1} \boldsymbol{e}_1}{\sqrt{\boldsymbol{e}_1^\top \Theta_{s_i,s_i}^{-1} \boldsymbol{e}_1}}$$

206 where the notation for Θ_{s_i,s_i}^{-1} is from (2.3) and $\boldsymbol{e}_1 \in \mathbb{R}^{|s_i| \times 1}$ denotes the vector with first entry
207 one and the rest zero. We enforce the convention that i is the first entry of s_i, also implying
208 that L is of full rank. Plugging the optimal L (2.11) back into the KL divergence (2.10),
209 we obtain the objective as a function of the sparsity pattern. See Appendix A.1 for details;
210 importantly, the order of the KL divergence matters.

211 (2.12)
$$2\mathbb{D}_{\mathrm{KL}}\Big(\mathcal{N}(\boldsymbol{0},\Theta) \,\Big\|\, \mathcal{N}(\boldsymbol{0},(LL^\top)^{-1})\Big) = \sum_{i=1}^{N} \left[\log\left(\Theta_{i,i|s_i \setminus \{i\}}\right) - \log\left(\Theta_{i,i|i+1:}\right) \right]$$

212 This sum is the accumulated *difference* in posterior variance for a series of independent
213 regression problems: each to predict the ith variable given a subset of the variables after it in
214 the ordering. The error $\log\left(\Theta_{i,i|s_i \setminus \{i\}}\right)$ made when restricted to the variables in the sparsity
215 pattern s_i is compared to the ground truth $\log\left(\Theta_{i,i|i+1:}\right)$. A similar decomposition of the KL
216 divergence into independent regression problems was observed in Equation (5) of [33] for lower
217 triangular transport maps.
218 Thus, picking the right sparsity pattern to minimize KL divergence reduces to selecting
219 the points s_i out of the possible candidates $i+1, \ldots, N$ that most reduce predictive error at
220 point(s) of interest. In the next section, we develop such a selection algorithm for directed
221 inference in Gaussian processes. We apply this algorithm for sparsity selection of sparse
222 Cholesky factors in section 4 and extend it in section 5.

223 **3. Greedy selection for directed inference.** In directed Gaussian process regression we
224 are given N points of training data and predict at a target point with unknown value by
225 selecting the s points most "informative" to the target, $s \ll N$. From KL-minimization, the
226 criterion for informativity should be to minimize the variance of the target point, conditional
227 on the selected points (2.12). The variance objective was first described by [13] for optimal
228 experimental design and later applied to directed Gaussian process inference by [21] who refer
229 to it as the active learning Cohn (ALC) technique in honor of [13]. In addition, the variance
230 objective is equivalent to maximizing the *mutual information* or *information gain* with the tar-
231 get point as well as minimizing the expected mean squared error (see subsection SM2.1). The
232 mutual information (in a slightly different context) is also used by [34] for sensor placement.
233 In contrast to Euclidean distance [61] or unconditional correlation [64, 30], conditional
234 variance incentivizes the often contradictory demands of being near the target point (nearby
235 points have higher covariance), but away from previously selected points (to avoid redun-
236 dancy); the resulting spread-out selections are illustrated in Figure 3. Even for isotropic
237 kernels like the Matérn family, the selections can be anisotropic, as shown in Figure 2.

238 **3.1. A greedy approach.** Minimizing the conditional variance over all possible $\binom{N}{s}$ subsets
239 is intractable, so we greedily select the next point which most reduces the conditional variance.
240 Let $I = \{i_j\}_{j=1}^t \subseteq \mathrm{Tr}$ be the indices of previously selected training points. For a newly selected
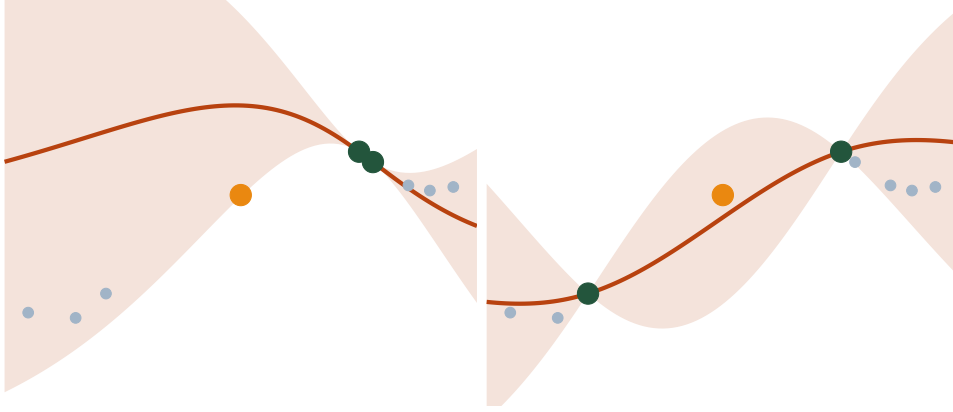
Figure 3. *Here, the blue points are the candidates, the orange point is the target point to predict at, and the green points are the selected points. The red line is the conditional mean μ, conditional on the selected points, and the $\pm 2\sigma$ confidence interval is shaded for the conditional variance σ^2. Each method has a budget of two points; the left panel shows selection by Euclidean distance and the right by conditional variance. Euclidean distance prefers the two points right of the target. However, a more balanced view of the situation is obtained when picking the slightly farther but more informative point to the left, reducing variance at the target and thereby reducing predictive error.*

index k, we condition the current covariance matrix on y_k according to the posterior (2.4), resulting in the rank-one downdate

$$(3.1) \qquad \Theta_{:,:|I,k} = \Theta_{:,:|I} - \boldsymbol{u}\boldsymbol{u}^\top \qquad\qquad \boldsymbol{u} = \frac{\Theta_{:,k|I}}{\sqrt{\Theta_{k,k|I}}}.$$

The decrease in the variance of y_{Pr} after selecting k is given by u_{Pr}^2, or

$$(3.2) \qquad u_{\mathrm{Pr}}^2 = \frac{\Theta_{\mathrm{Pr},k|I}^2}{\Theta_{k,k|I}} = \frac{\mathbb{Cov}[y_{\mathrm{Pr}}, y_k \mid I]^2}{\mathbb{Var}[y_k \mid I]} = \mathbb{Corr}[y_{\mathrm{Pr}}, y_j \mid I]^2 \, \mathbb{Var}[y_{\mathrm{Pr}} \mid I].$$

To compute the objective (3.2) for each candidate index j, we start with the unconditional variance $\Theta_{j,j}$ and covariance $\Theta_{\mathrm{Pr},j}$, updating these quantities when an index k is selected by Equation (3.1). We have two efficient strategies to compute $\boldsymbol{u}$ (as shown in Figure 4): either by maintaining the precision of selected entries $\Theta_{I,I}^{-1}$ (Algorithm SM3.1) or by storing only the $|I|$ columns corresponding to selected points from the Cholesky factor of the joint covariance matrix Θ (Algorithm SM3.2); both methods are detailed in subsection SM3.1.

Both approaches have a time complexity of $\mathcal{O}(Ns^2)$ to select s points out of N candidates, differing in space complexity. The precision takes $\mathcal{O}(s^2)$ space while the first s columns of the Cholesky factor of Θ uses $\mathcal{O}(Ns)$ space, always more memory ($N > s$). Both algorithms use $\mathcal{O}(N)$ space to store the conditional (co)variances. The precision algorithm uses less memory than the Cholesky algorithm. However, the Cholesky algorithm is easier to implement and roughly two times faster, which is why we use it in practice.

4. Greedy selection for global approximation by KL-minimization. Directed Gaussian process regression infers the *local* distribution at points of interest. We now turn our attention

Algorithm 3.1 Point selection update by explicit precision

Input: $X = \begin{pmatrix} X_{\text{Tr}} \\ X_{\text{Pr}} \end{pmatrix}, K(\cdot, \cdot), I, \Theta_{:,:|I}, \Theta_{I,I}^{-1}, k$

1: $I \leftarrow I \cup \{k\}$
2: $\boldsymbol{v} \leftarrow \Theta_{I,I}^{-1} K(X_{I\setminus\{k\}}, X_k)$
3: $\Theta_{I,I}^{-1} \leftarrow \begin{pmatrix} \Theta_{I,I}^{-1} + \boldsymbol{v}\boldsymbol{v}^\top/\Theta_{k,k|I} & -\boldsymbol{v}/\Theta_{k,k|I} \\ -\boldsymbol{v}^\top/\Theta_{k,k|I} & 1/\Theta_{k,k|I} \end{pmatrix}$
4: $\Theta_{:,k} \leftarrow K(X, X_k)$
5: $\Theta_{:,k|I} \leftarrow \Theta_{:,k} - K(X, X_{I\setminus\{k\}})\boldsymbol{v}$
6: $\boldsymbol{u} \leftarrow \frac{\Theta_{:,k|I}}{\sqrt{\Theta_{k,k|I}}}$
7: **for** $j \in \text{Tr} \setminus I$ **do**
8: $\quad \Theta_{j,j|I} \leftarrow \Theta_{j,j|I} - \boldsymbol{u}_j^2$
9: $\quad \Theta_{j,\text{Pr}|I} \leftarrow \Theta_{j,\text{Pr}|I} - \boldsymbol{u}_j\boldsymbol{u}_{N+1}$
10: **end for**

Algorithm 3.2 Point selection update by Cholesky factorization

Input: $X = \begin{pmatrix} X_{\text{Tr}} \\ X_{\text{Pr}} \end{pmatrix}, K(\cdot, \cdot), I, \Theta_{:,:|I}, L, k$

1: $I \leftarrow I \cup \{k\}$
2: $i \leftarrow |I|$
3: $L_{:,i} \leftarrow K(X, X_k)$
4: $L_{:,i} \leftarrow L_{:,i} - L_{:,:i-1}L_{k,:i-1}^\top$
5: $L_{:,i} \leftarrow \frac{L_{:,i}}{\sqrt{L_{k,i}}}$
6: **for** $j \in \text{Tr} \setminus I$ **do**
7: $\quad \Theta_{j,j|I} \leftarrow \Theta_{j,j|I} - L_{j,i}^2$
8: $\quad \Theta_{j,\text{Pr}|I} \leftarrow \Theta_{j,\text{Pr}|I} - L_{j,i}L_{N+1,i}$
9: **end for**

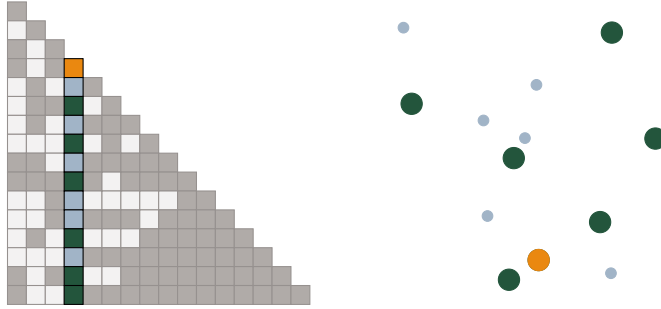**Figure 4.** *Algorithms for updates in single-target selection.*

Figure 5. *For a column of a Cholesky factor in isolation, the* target *point is the* diagonal *entry,* candidates *are* below *it, and the* selected *entries are added to the* sparsity pattern. *Points violating lower triangularity are not shown. Thus, sparsity selection in Cholesky factorization (left panel) is analogous to training point selection in directed Gaussian process regression (right panel).*

to *global* approximation of the entire Gaussian process; given a kernel function $K(\boldsymbol{x}, \boldsymbol{x}')$ and a set of N points $\{\boldsymbol{x}_i\}_{i=1}^N$ we have the covariance matrix $\Theta_{ij} = K(\boldsymbol{x}_i, \boldsymbol{x}_j)$ for which we seek a sparse approximate Cholesky factor L of the precision, $LL^\top \approx \Theta^{-1}$. We first order the points by the reverse-maximin ordering described in subsection 2.2 and then apply the selection algorithm developed in section 3 to form the sparsity pattern. For the ith column of L, the target point is the ith point in the ordering, the candidate points are those satisfying lower triangularity (after the target in the ordering), and running the selection algorithm for the desired number of nonzeros entries picks out indices which we add to the sparsity set s_i; this process is illustrated in Figure 5. Finally, we compute the values of the selected nonzero indices by the closed-form expression (2.11). Both sparsity selection and computing entries

are embarrassingly parallel over L's columns.

Using the single-target algorithm from subsection 3.1 has time complexity $\mathcal{O}(NCs^2)$ to select s nonzero entries out of C candidates for N columns. Computing the corresponding values $\Theta_{s_i,s_i}^{-1}\boldsymbol{e}_1$ has time complexity $\mathcal{O}(Ns^3)$. Sparsity selection has the same complexity as entry computation if the number of candidates C is $\mathcal{O}(s)$, suggesting the need to limit the number of candidates considered. In practice, we pick the candidate set to be the nearest neighbors of the point of interest as [21] does; specifically, we use the framework of [47] which considers all points within a radius proportional to the length scale from the reverse-maximin ordering (2.8).

5. Extensions. Here we consider extensions of the basic single-column method to aggregated (or supernodal) Cholesky factorization and to determining the number of nonzeros per column. Numerical experiments are presented in section 6.

5.1. Aggregated sparsity pattern. We now derive a similar decomposition of the KL divergence if the same sparsity pattern is reused for multiple columns, known as aggregated or supernodal Cholesky factorization. Aggregation can lead to substantial time and space savings [47]. For this section we focus on a single group $\tilde{i} = \{i_1, \ldots, i_m\}$ obtained by aggregating the column indices $i_1 \succ i_2 \succ \cdots \succ i_m$. Let $\tilde{i}$ have aggregated selected entries $s_{\tilde{i}}$ satisfying $s_{\tilde{i}} \supseteq \tilde{i}$ to guarantee that the Cholesky factor has full rank. Let $\tilde{s} := s_{\tilde{i}} \setminus \tilde{i}$ be the selected entries excluding the columns in the group. The sparsity pattern for the kth column in the group is then the aggregated selected entries excluding the entries that violate lower triangularity, $s_k := \{j \in s_{\tilde{i}} : j \succeq k\}$. Assuming every entry of $\tilde{s}$ is after every index in $\tilde{i}$, then $s_k = \tilde{s} \cup \{j \in \tilde{i} : j \succeq k\}$. This condition is guaranteed if the aggregated columns are adjacent in the ordering, for example; we defer handling the general case to the next section. The KL divergence (2.12) restricted to the contribution from the group $\tilde{i}$ is

$$(5.1) \qquad \sum_{i \in \tilde{i}} \log\left(\Theta_{i,i|s_i \setminus \{i\}}\right) = \mathrm{logdet}(\Theta_{\tilde{i},\tilde{i}|\tilde{s}})$$

from Appendix A.2. Thus, the generalization of the posterior variance (2.12) to aggregated columns is their log determinant conditional on (well-behaved) selected entries. We briefly discuss what happens when selected entries are *between* columns.

5.1.1. Nonadjacent or partial aggregation. Let the random variables corresponding to the indices $\tilde{i} = \{i_1, \ldots, i_m\}$ be collected in a vector $\boldsymbol{y} = [y_1, \ldots, y_m]^\top$ with joint density $\boldsymbol{y} \sim \mathcal{N}(\boldsymbol{0}, \Theta)$. We select a random variable with index k and define *partial* conditioning to mean that k conditions all but the first p variables (recall that the indices are sorted w.r.t $\succ$, so if k conditions a variable, it conditions all those afterwards). We denote the partial conditioning of y as $\boldsymbol{y}_{\|k} := [y_1, \ldots, y_p, y_{p+1|k}, \ldots, y_{m|k}]^\top$ and its covariance matrix $\mathbb{Cov}[\boldsymbol{y}_{\|k}]$ as

$$(5.2) \qquad \Theta_{\tilde{i},\tilde{i}\|k} := \mathbb{Cov}[\boldsymbol{y}_{\|k}] = \begin{pmatrix} L_{:p}L_{:p}^\top & L_{:p}L'^\top_{p+1:} \\ L'_{p+1:}L_{:p}^\top & L'_{p+1:}L'^\top_{p+1:} \end{pmatrix} = \begin{pmatrix} L_{:p} \\ L'_{p+1:} \end{pmatrix} \begin{pmatrix} L_{:p} \\ L'_{p+1:} \end{pmatrix}^\top$$

305 where $L = \text{chol}(\Theta)$ and $L' = \text{chol}(\Theta_{:,:|k})$. See Figure 17 for an illustration and Appendix A.3
306 for details. Armed with this representation, we compute $\text{logdet}(\Theta_{\tilde{i},\tilde{i}\|k})$:

307 (5.3)
$$\sum_{i \in \tilde{i}} \log\left(\Theta_{i,i|s_i \setminus \{i\}}\right) = \text{logdet}(\Theta_{\tilde{i},\tilde{i}\|k}).$$

308 Like the aggregated case (5.1), minimizing the log determinant of the *partially* conditioned
309 covariance matrix (5.2) is the same as minimizing the KL divergence (2.12).

310 **5.2. Supernodes and blocked selection.** For multiple $(m > 1)$ target points, [21] suggests
311 independently applying the single-target algorithm to each target. Instead, we will use *the*
312 *same* selected points for *all* the target points, essentially speeding up selection by a factor
313 of m. Furthermore, the cost of computing the entries of the resulting Cholesky factor is
314 reduced by this aggregation. The primary downside is reduced accuracy per sparsity entry
315 since each target no longer receives individual attention. We mitigate this by paying heed to
316 the "two birds with one stone" maxim, or by considering a candidate's simultaneous effect
317 on *all* prediction points. In practice, this approach yields better accuracy per unit time than
318 single-target selection.
319   The first question is how to generalize the objective for a single target (3.2) to multiple
320 targets. Continuing with KL-minimization (5.1), the criterion should be to minimize the log
321 determinant of the posterior covariance matrix, $\text{logdet}(\Theta_{\text{Pr},\text{Pr}|I})$. This objective, known as D-
322 optimal design in the literature [34], can be intuitively interpreted as a volume of uncertainty
323 or as a scaling factor in the density of multivariate Gaussians. In addition, it is equivalent to
324 maximizing mutual information since the differential entropy of a Gaussian strictly increases
325 with its log determinant (see subsection SM2.1).
326   We want to quickly compute how selecting an index k affects the log determinant. By
327 application of the matrix determinant lemma (the details are in subsection SM2.5),

328 (5.4) $\text{logdet}(\Theta_{\text{Pr},\text{Pr}|I,k}) - \text{logdet}(\Theta_{\text{Pr},\text{Pr}|I}) = \log(\Theta_{k,k|I,\text{Pr}}) - \log(\Theta_{k,k|I}).$

329 Equation (5.4) swaps the roles of the targets and the candidate: the *candidate* is now con-
330 ditioned by the *targets*, reducing to single-target selection. Using the recipes from subsec-
331 tion 3.1 to compute conditional variances, we can compute the objective by maintaining a
332 data structure for each term: one for $\Theta_{k,k|I,\text{Pr}}$ and the other for $\Theta_{k,k|I}$. By the quotient rule
333 $\Theta_{k,k|I,\text{Pr}} = \Theta_{k,k|\text{Pr},I}$, so we can condition on the prediction points *before* any points have been
334 selected. After this initialization, we repeatedly update both data structures after selecting
335 the best candidate by the objective (5.4).
336   We have two strategies from the two approaches of the single-target algorithm: one main-
337 taining the precision of the selected entries $\Theta_{I,I}^{-1}$ as well as of the target points $\Theta_{\text{Pr},\text{Pr}}^{-1}$ (Algo-
338 rithm SM3.4) and the other simply storing two Cholesky factors of the joint covariance matrix
339 Θ (Algorithm SM3.5); both methods are detailed in subsection SM3.2.
340   Both approaches have a time complexity of $\mathcal{O}(Ns^2 + Nm^2 + m^3)$ to select s points out of
341 N candidates for m targets, again differing in space complexity: although using more memory,
342 the Cholesky approach is preferred for simplicity and performance.

Partial selection. The multiple-target algorithm implicitly assumes that a candidate conditions *every* target point. However, candidates can also condition only a subset of the targets in the aggregated Cholesky factorization setting of subsection 5.1.1. Proper "partial" selection accounting for this structure is able to match the asymptotic time and space complexities of the multiple-target algorithm by also storing a partial Cholesky factor, the details are provided in subsection SM3.3 and Algorithm SM3.7.

5.3. Aggregated Cholesky. In an aggregated sparsity pattern, columns are partitioned into groups and selecting an index for a group $\tilde{i}$ adds it to the sparsity.

We group columns by the framework of [47] which aggregates points that are close both geometrically as well as in the ordering. To select sparsity entries, the targets are all points in $\tilde{i}$ and the candidates are the union of the nearest neighbors to each target. If every candidate k satisfies $k \succ \max \tilde{i}$ which occurs if the group is contiguous in the ordering e.g., then every candidate conditions every target and so the multiple-target selection algorithm (subsection 5.2) can be directly applied. However, we empirically observe that forcing this condition irreparably damages the accuracy of the resulting factor: forming groups contiguous in the ordering no longer guarantees that grouped points are spatially close, and removing candidates between targets filters many of them out. If the condition is not forced, then selecting candidates can condition subsets of the group; the multiple-target algorithm now systematically overestimates the effect on targets. Using the partial selection algorithm (subsection SM3.3) instead on unmodified grouping and candidate sets significantly improves the approximation quality.

Because the sparsity patterns for columns in the same group are subsets of each other, we can efficiently compute the group's entries in L (2.11) together in the time complexity for a single column (see subsection SM1.1 or Algorithm 3.2 of [47]). If each group has m points, both the multiple-target and partial algorithms have time complexity $\mathcal{O}(Cs^2 + Cm^2 + m^3)$ to select s points out of C candidates. Over N/m groups the time complexity for both selection and entry computation is $\mathcal{O}(\frac{N}{m}(Cs^2 + Cm^2 + m^3 + s^3))$, simplifying to $\mathcal{O}(\frac{NCs^2}{m})$ assuming $m = \mathcal{O}(s)$, a m times improvement over non-aggregated factorization. Better time complexity yields denser and thereby more accurate factors in the same amount of time. However, the sparsity pattern is no longer tailored to particular columns since it is shared within a group. This means the aggregated factor is less efficient at reducing the KL divergence per nonzero.

5.4. Allocating nonzeros by global greedy selection. Given a budget on the total number of nonzeros, one must decide how many nonzeros to assign to each column. We recommend the simple strategy of distributing nonzeros as evenly as possible, maximizing computational efficiency since denser columns have an outsized impact on the computational time from the cubic scaling cost with the number of nonzeros.

In inhomogeneous geometries where certain points benefit from more nonzeros than others, a principled way of distributing nonzeros is to minimize KL divergence end-to-end like was done for sparsity selection. The *local* greedy algorithms select the sparsity entry that minimizes prediction error at *particular* columns of interest. In *global* greedy selection, we pick from *any* column the candidate that minimizes the overall KL divergence (2.12). We maintain a priority queue containing all candidates from every column, keyed by the candidate's effect on the KL divergence. The data structure must support popping the largest element off the queue as

386 well as updating the value for an element in the queue. Both operations have time complexity
387 $\mathcal{O}(\log n)$ for n elements if implemented as an array-backed binary heap, for example.
388   The greedy selection algorithms already compute the effect of an entry on the KL diver-
389 gence, up to monotonically increasing transformations (which preserve the ranking of candi-
390 dates). But in the global context, if different columns use different transformations, then the
391 ranking of candidates between columns is skewed. We describe the necessary modifications to
392 compute exactly the difference in KL divergence.

393   **5.4.1. Single column selection.** Selecting an entry k for a single target only affects its
394 conditional variance, so exactly one term in the KL divergence (2.12) changes,

395 (5.5) $$\underset{k}{\operatorname{argmin}} \left[\log(\Theta_{\mathrm{Pr},\mathrm{Pr}|I,k}) - \log(\Theta_{\mathrm{Pr},\mathrm{Pr}|I}) \right] = \underset{k}{\operatorname{argmin}} \left(\Theta_{\mathrm{Pr},\mathrm{Pr}|I,k} \right) \Theta_{\mathrm{Pr},\mathrm{Pr}|I}^{-1}.$$

396 Using the original objective (3.2) to compute the change in variance from selecting k,

397 (5.6) $$\underset{k}{\operatorname{argmin}} \left(\Theta_{\mathrm{Pr},\mathrm{Pr}|I} - \frac{\Theta_{\mathrm{Pr},k|I}^2}{\Theta_{k,k|I}} \right) \Theta_{\mathrm{Pr},\mathrm{Pr}|I}^{-1} = \underset{k}{\operatorname{argmax}} \ \mathbb{C}\mathrm{orr}[y_{\mathrm{Pr}}, y_k \mid I]^2$$

398 where the new objective (5.6) is easily computed as the original objective (3.2) divided by the
399 target's conditional variance, the percentage the decrease in variance takes up.

400   **5.4.2. Aggregated selection.** The multiple-target algorithm already computes the exact
401 difference in log determinant after selecting a candidate. The partial selection algorithm
402 computes the log determinant itself, not the difference, so the log determinant before the
403 selection needs to be subtracted, easily computed as the sum of the squared "diagonal" entries
404 of L corresponding to target points from (SM3.2).

405   **6. Numerical experiments.** All experiments ran on the Partnership for an Advanced
406 Computing Environment (PACE) Phoenix cluster at the Georgia Institute of Technology, with
407 8 cores of a Intel Xeon Gold 6226 CPU @ 2.70GHz and 22 GB of RAM per core. The code is
408 written in Python using standard scientific libraries `numpy` [26], `scipy` [63], `scikit-learn` [41],
409 `matplotlib` [29] as well as Cython [5] which provides direct transpilation of Python code into
410 C. Cython also allows Python code to access native C interfaces to the `BLAS` and Intel `oneMKL`
411 libraries. Code for all numerical experiments can be found at https://github.com/stephen-
412 huan/conditional-knn.

413   **6.1. Cholesky factorization.** We empirically verify that conditional sparsity selection pro-
414 duces more accurate sparse Cholesky factors than selection by Euclidean distance at the same
415 density. We take N points on a slightly perturbed regular grid in $[0,1]^2$ and use a Matérn
416 kernel with smoothness $\nu = 5/2$ and length scale $\ell = 1$.
417   As a baseline for comparison, we use the single-column and aggregated variants of the
418 KL-minimization framework of [47], which orders points by the reverse-maximin ordering
419 described in subsection 2.2 and forms the sparsity pattern by selecting all points within a
420 radius of $\rho \ell_i$ to the ith point, where $\rho \geq 1$ is a tuning parameter for density and ℓ_i is the
421 length scale from the reverse-maximin ordering. We also try selecting points by k-nearest
422 neighbors (k-NN), where k is chosen to match the number of nonzeros of the baseline.
423   For our method, we run the baseline with a larger $\rho' = \rho_s \cdot \rho$ to get an initial candidate
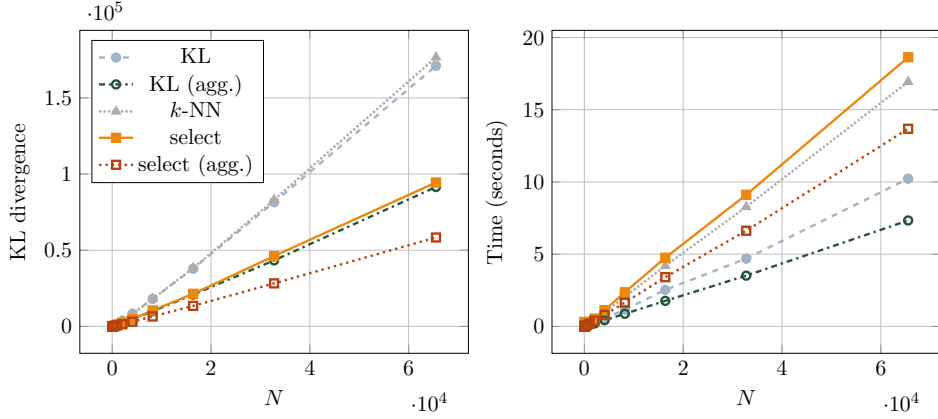424 set where ρ_s is a tuning parameter for the number of candidates considered. If not stated

Figure 6. *Accuracy (left) and computational time (right) of Cholesky factorization methods with varying number of points N and fixed density $\rho = 2$. "KL" is the baseline from [47], "k-NN" is selection by k-nearest neighbors, "select" is conditional selection, and "(agg.)" denotes aggregation.*

otherwise, $\rho_s = 2$ is used in the following experiments. We then use the single-column and partial variants of the conditional selection algorithm described in section 3 to subsample the actual sparsity entries from the candidate set; in these experiments, each column receives k nonzeros where k is chosen to match the original density ρ of the baseline factor. In this setting we found that using the global selection procedure described in subsection 5.4 to determine the number of nonzeros for each column led to little improvement in accuracy at a significant performance penalty.

We aggregate columns by the procedure of [47]: pick the first (w.r.t $\prec$) index i that has not been aggregated and create the group $\{j : j \in s_i, \ell_j \leq \lambda \ell_i\}$ where $\lambda \geq 1$ is a tuning parameter for group size; repeat until all indices have been aggregated. We generate the groups using the sparsity pattern from the baseline factor and use the same groups for aggregated conditional selection for a fair comparison. In all experiments we use $\lambda = 1.5$ as recommended by [47].

As Figure 6 shows, the KL divergence and computational time increase linearly with the number of points for all methods. Conditional methods are more accurate than their unconditional counterparts and the denser aggregated variants are both more accurate and faster than their non-aggregated counterparts.

Figure 7 shows that the conditional selection methods achieve significantly better KL divergence compared to their unconditional counterparts for the same number of entries of the sparsity set. However, they do not achieve better accuracy per unit time cost from the increased cost of selection. Aggregation results in better accuracy per unit time cost but worse accuracy per nonzero entry, which may impact their computational efficiency in downstream tasks which depend on factor density like preconditioning.

6.2. Gaussian process regression. For Gaussian process regression we use the "predictions points first" method of [47] which computes a sparse Cholesky factor of the joint covariance matrix between the training and prediction points, where prediction points are ordered before training points. The desired posterior mean and covariance can then be computed efficiently from sparse submatrices of the factor. See subsection 4.2.1, Appendix D.1, or
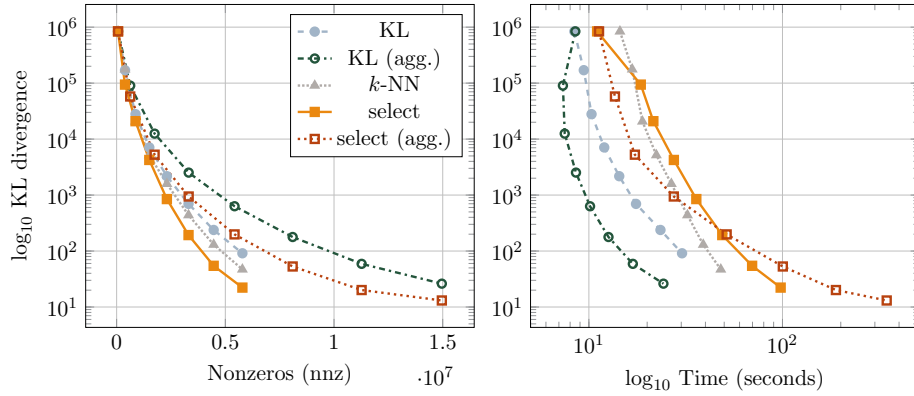
Figure 7. *The left panel shows the KL divergence with varying density ρ and the right panel shows the accuracy to computational time trade-off over varying ρ. The number of points is $N = 2^{16}$.*
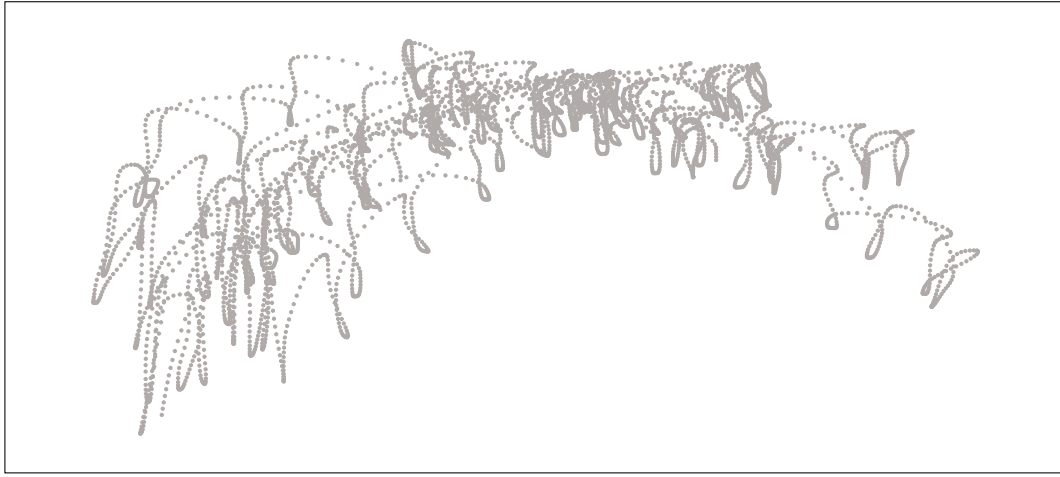

Figure 8. *The first 5,000 points of the SARCOS training data, visualizing the first two features.*

Algorithm D.1 of [47] for additional details.

6.2.1. SARCOS dataset. We use the SARCOS dataset [62] generated from an inverse dynamics problem on a 7 degrees-of-freedom robotic arm. Given 7 joint positions, velocities, and accelerations for 21 features in total, the goal is to infer the torque of just the first joint. The dataset is available online at https://gaussianprocess.org/gpml/data/ and consists of 44,484 training points and 4,449 testing points which we then preprocess as follows.

We only use the first 3 features of the data and remove the 73 duplicate points this projection causes. Since the provided testing points overlap significantly with the training points, we ignore the original testing points and instead randomly partition the 44,411 remaining training points into 90% training points ($N = 39,969$) and 10% prediction points ($m = 4,442$). Since the robot arm moves smoothly, the geometry of the dataset consists of relatively continuous overlapping paths as shown in Figure 8. We then use a Matérn kernel with smoothness $\nu = 3/2$ and length scale $\ell = 1$ and draw 10^3 realizations from the resulting Gaussian process
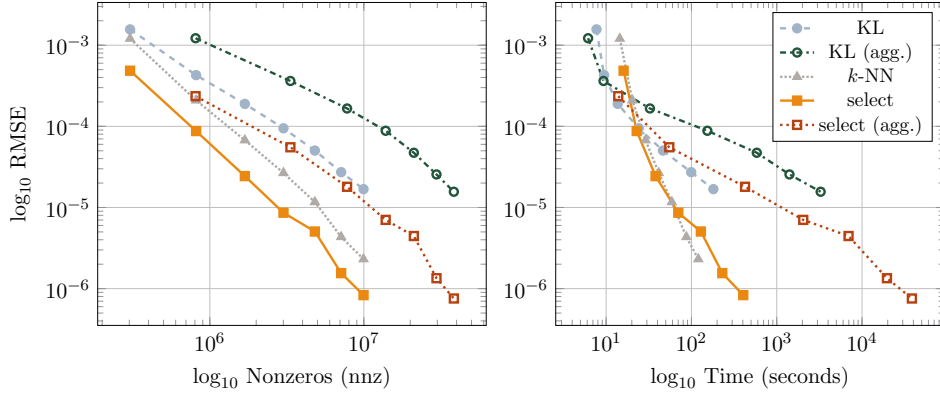
Figure 9. *We perform Gaussian process regression by sparse Cholesky factorization of the joint covariance matrix. Like Cholesky factorization in subsection 6.1, we use a candidate set size scaling factor of $\rho_s = 2$ and an aggregation parameter of $\lambda = 1.5$. The left panel shows the difference in RMSE from exact Gaussian process regression using the same training points with varying density ρ. The right panel shows the accuracy to computational time trade-off over varying ρ.*

for the target variable, ignoring the original objective to ensure that the target variable is exactly Gaussian.

We consider three accuracy metrics for Gaussian process regression: the log determinant of the posterior prediction covariance matrix, the empirical coverage of the 90% posterior prediction intervals averaged over all realizations, and the average root mean square error (RMSE) of the posterior means. The log determinant is equivalent to the KL divergence by the discussion in subsection 5.1, so the results are similar to Cholesky factorization (subsection 6.1). We find that coverage is extremely accurate for all methods (within 0.1% for $\rho > 2$). Finally, the RMSE is shown in Figure 9.

Despite an increased cost to select points, the conditional methods have better accuracy per unit computational cost than their unconditional counterparts as a result of their superior accuracy at the same sparsity. However, the simpler method of k-NN also achieves comparable accuracy per unit time cost. As noted in [22], the simple method of k-NN remains hard to beat without specialized tricks.

6.2.2. OCO-2 dataset. We also use data produced by the OCO-2 project [14] at the Jet Propulsion Laboratory, California Institute of Technology, obtained from the OCO-2 data archive maintained at the NASA Goddard Earth Science Data and Information Services Center which is available online at https://disc.gsfc.nasa.gov/datasets?keywords=oco2. OCO-2 is an orbiting satellite designed to measure atmospheric carbon dioxide. The path an orbiting satellite takes creates characteristic streaks in the data as shown in Figure 10.

We take data localized to the United States from the time period 2017-05-16 to 2017-05-31, keeping only the features of longitude, latitude, and time and removing any duplicates points. We then take the first 2^{16} points and draw 10^3 realizations from the Gaussian process with the same train test split, kernel function, and hyperparameters as the SARCOS experiment.

As shown in Figure 11, the RMSE of k-NN is worse than the "KL" baseline. However, in every other experiment (Figure 7, Figure 9, and Figure 12) k-NN does better than the
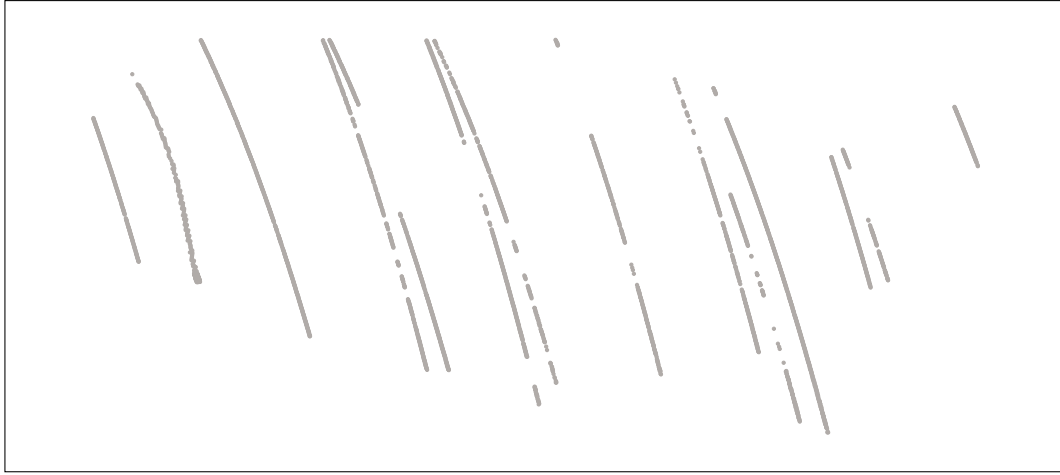
Figure 10. *Sampling 4,682 evenly spaced points from the OCO-2 dataset, visualizing the first two features.*
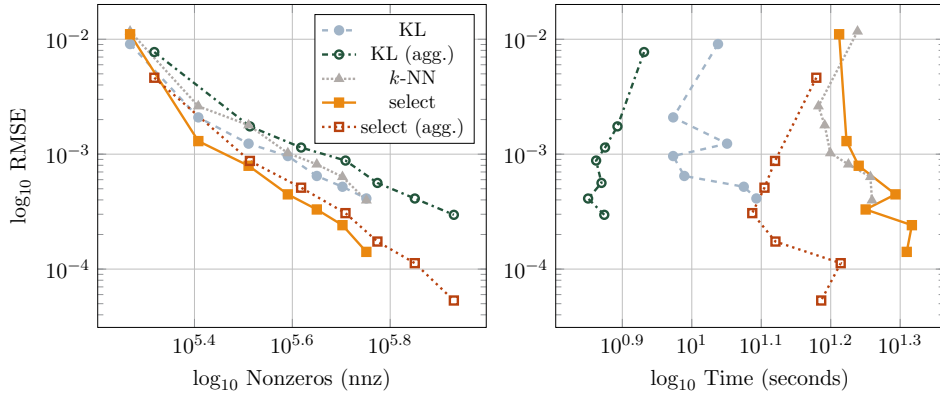

Figure 11. *We use a candidate set size scaling factor of $\rho_s = 2$ and an aggregation parameter of $\lambda = 1.5$. The left panel shows the difference in RMSE from exact Gaussian process regression with varying density ρ. The right panel shows the accuracy to computational time trade-off over varying ρ.*

baseline, so neither method is strictly better than the other. Our method, on the other hand, achieves the best accuracy in *every* numerical experiment over a wide variety of geometries and tasks, a testament to its robustness.

6.3. Preconditioning for conjugate gradient. Motivated by the equivalence of functionals like the Kaporin condition number to the KL divergence, we investigate solving symmetric positive-definite systems $\Theta x = y$ using the conjugate gradient and a sparse Cholesky factor L as a preconditioner. We note that from (2.10) the KL divergence strongly penalizes zero eigenvalues of the preconditioned matrix $\Theta L L^\top$, improving its condition number. In order to generate the covariance matrix Θ we sample up to $N = 2^{16}$ points uniformly at random from the unit cube $[0,1]^3$ and use a Matérn kernel with smoothness $\nu = 1/2$ and length scale $\ell = 1$. In exploratory numerical experiments, we found using higher smoothnesses like $\nu = 5/2$ led to extremely poor condition numbers and numerical instability (over thousands
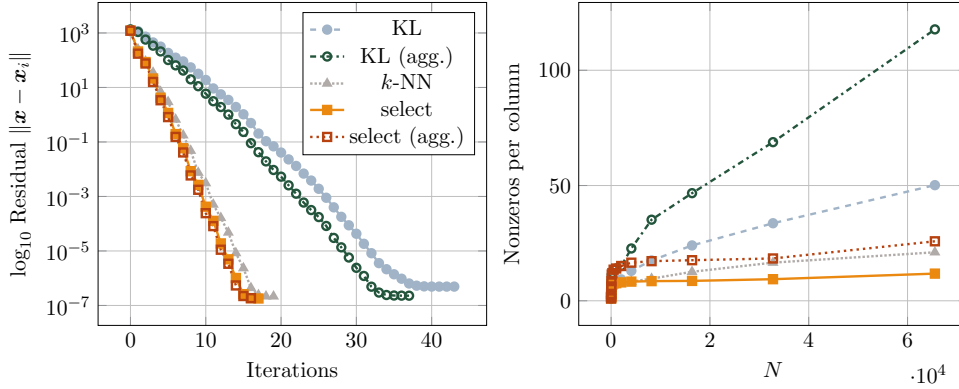
Figure 12. *We use the conjugate gradient preconditioned by sparse Cholesky factors to solve the symmetric positive-definite system $\Theta \boldsymbol{x} = \boldsymbol{y}$. The left panel shows iteration progress for $N = 2^{16}$ points and a factor density of $\rho = 4$. The right panel shows the minimum number of nonzeros per column for conjugate gradient to converge within 50 iterations with an increasing number of points.*
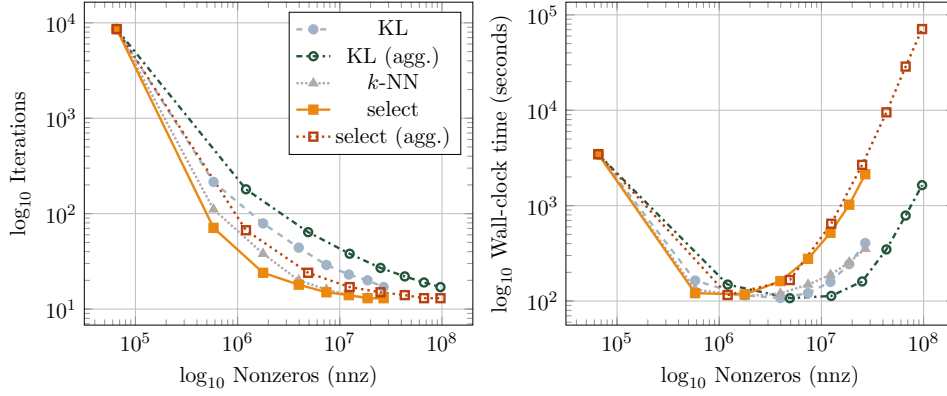

Figure 13. *The left panel shows how the number of iterations for the conjugate gradient to converge decreases with increasing preconditioner density ρ for $N = 2^{16}$ points. The right panel shows the total wall-clock time (both to compute the preconditioner and to converge) with varying density.*

503 of iterations to converge). Increasing length scale also worsens the condition but to a less
504 extreme extent. Rather than generate a right-hand side $\boldsymbol{y}$ directly, we first sample a solution
505 $\boldsymbol{x} \sim \mathcal{N}(\boldsymbol{0}, \mathrm{Id}_N)$ and then compute $\boldsymbol{y} = \Theta \boldsymbol{x}$ so that $\boldsymbol{y}$ is realistically smooth. When computing
506 the preconditioner L by sparse Cholesky factorization, we use a candidate set size scaling
507 factor of $\rho_s = 2$ and an aggregation parameter of $\lambda = 1.5$. We then run the conjugate gradient
508 algorithm with L as a preconditioner until reaching a relative tolerance of 10^{-12}.

509   As shown in Figure 12, the conditional methods converge in half the iterations of their
510 unconditional counterparts and aggregation barely reduces the number of iterations. The
511 minimum number of nonzeros per column to converge within a constant number of iterations
512 (here, 50) seems to grow logarithmically with the number of points for all methods; although
513 the conditional methods appear near constant.

514   We observe a characteristic "U" shape for the total wall-clock time in Figure 13 from the
515 trade-off between spending computational time in forming the preconditioner or in conjugate
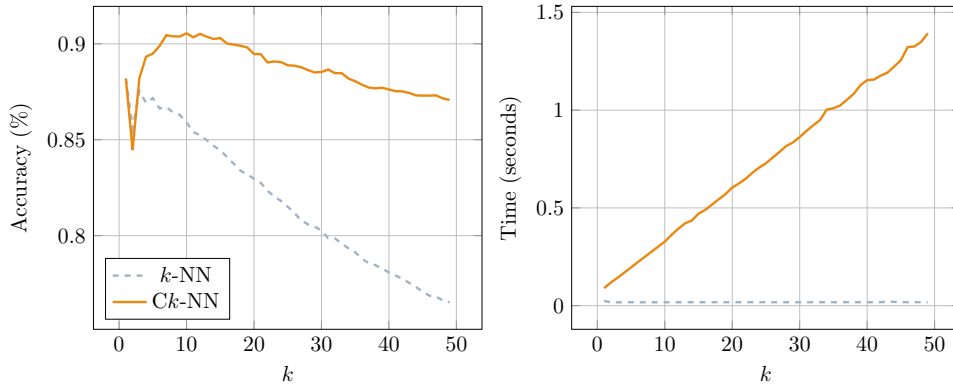
Figure 14. *We compare selection by Euclidean distance (k-NN) to conditional selection (Ck-NN) in image classification. From the MNIST database $N = 10^3$ training images and $m = 10^2$ testing images are randomly chosen; each test image is classified by the mode label of k selected images, and this process is repeated 10^2 times for each value of k. (Left:) Accuracy with k. (Right:) the time to select k points using Ck-NN seems to scale linearly with k although it is quadratic asymptotically; possibly resulting from applying highly optimized BLAS operations to relatively small matrices.*

516 gradient iterations. Across all preconditioner densities, the aggregated variants are slower
517 than their non-aggregated counterparts due to barely reducing the number of iterations while
518 producing significantly denser factors with slower matrix-vector products. The time-optimal
519 density for conditional methods is sparser than their unconditional counterparts due to using
520 fewer iterations at the same sparsity and it being more expensive to select nonzeros. It is hard
521 to directly compare the total computational time of the methods because simply increasing
522 the number of iterations, e.g., by demanding better tolerance or by using matrices with worse
523 condition numbers, will prefer more accurate methods even if they are slower to form the
524 preconditioner.

525   **6.4. k-nearest neighbors selection.** We compare k-nearest neighbors (k-NN) to our se-
526 lection algorithm from subsection 3.1, which we call conditional k-nearest neighbors (Ck-NN),
527 in the following toy example performing image classification. From the MNIST database of
528 handwritten digits [35], we randomly select $N = 10^3$ training images and $m = 10^2$ testing
529 images. We classify a test image by selecting k training images and taking the mode label
530 of those images. For k-NN, we use the Euclidean distance and for Ck-NN, we use a Matérn
531 kernel with smoothness $\nu = 3/2$ and length scale $\ell = 2^{10}$. Accuracy is the percentage of test
532 images classified correctly.

533   The accuracy of both methods decreases linearly with increasing k as shown in Figure 14.
534 We hypothesize that nearby images are more likely to have the same label, so selecting more
535 points increases the influence of further, differently labeled images. Ck-NN remains more
536 accurate than k-NN for every $k > 2$, suggesting it consistently selects more informative im-
537 ages. We emphasize that conditioning alone causes the difference in accuracy: unconditional
538 covariance decays monotonically with distance.

539   **6.5. Recovery of sparse Cholesky factors.** Motivated by the similarity of the selection
540 algorithm to orthogonal matching pursuit [59], we attempt to recover an *a priori* sparse
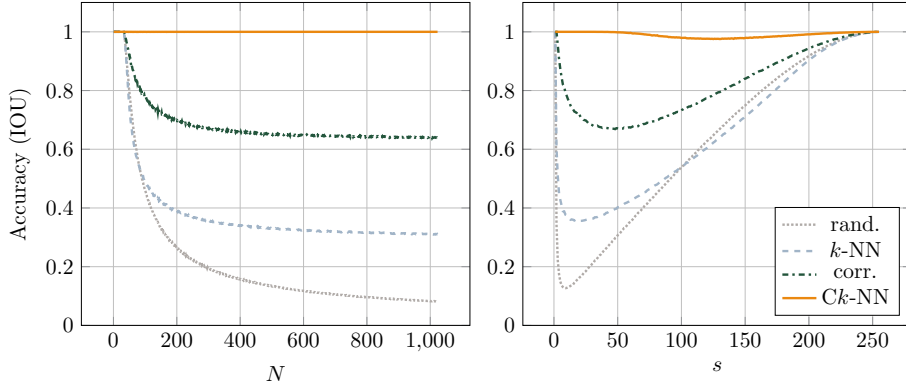
Figure 15. *We attempt to recover a sparse Cholesky factor L of the precision matrix $Q = LL^\top$. "Ck-NN" minimizes the conditional variance of the target (diagonal) entry, "corr." maximizes correlation with the target, "k-NN" maximizes covariance with the target, and "rand." samples entries uniformly at random. All methods achieve their best accuracy given Q except Ck-NN which is given the covariance matrix Q^{-1}. (Left:) Varying the size of L, fixed density $s = 2^5$. (Right:) Varying s, fixed size $N = 2^8$. Accuracy starts to improve from the factor nearing fully dense.*
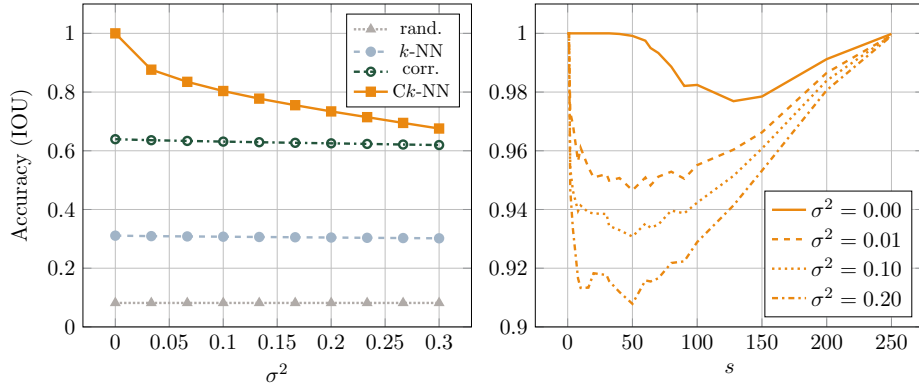

Figure 16. *We add noise sampled i.i.d. from $\mathcal{N}(0, \sigma^2)$ to the measurements Q. The left panel shows accuracy with varying noise for $N = 2^{10}$ columns and $s = 2^5$ nonzeros per column. The right panel shows accuracy for the Ck-NN method at various noise levels for $N = 2^8$ and varying s.*

Cholesky factor L from its precision matrix $Q = LL^\top$. To generate the nonzero entries of L, for each column we pick s lower triangular indices uniformly at random and sample their values i.i.d. from $\mathcal{N}(0, 1)$. We fill L's diagonal with a "large" positive value 10 to ensure Q is well-conditioned. The selection algorithm is given s and either Q or the covariance matrix Q^{-1} depending on which results in higher accuracy in reconstructing L. For a recovered sparsity pattern X and ground truth Y we report $|X \cap Y|/|X \cup Y|$, the intersection over union (IOU). Using the KL divergence (2.9) of the recovered Cholesky factor seems mostly equivalent to IOU.

As shown in Figure 15, Ck-NN maintains a near-perfect recovery accuracy much higher than the unconditional baselines. In the setting of noisy measurements, noise sampled i.i.d from $\mathcal{N}(0, \sigma^2)$ is symmetrically added to each entry of Q ($Q_{i,j}$ receives the same noise as $Q_{j,i}$).

Accuracy degrades with increasing noise for all methods, but Ck-NN is the most sensitive to noise as is shown in Figure 16. At high enough levels of noise Q can lose positive-definiteness, causing Ck-NN to break down entirely.

7. Comparisons and conclusion. We briefly compare our method to prior works.

7.1. Comparison to other methods.

Local approximate Gaussian process (laGP). Our conditional variance objective for point selection (3.2) was first described in [13] for optimal experimental design, and has subsequently been named the active learning Cohn (ALC) technique. [21] and the follow-up works [22, 57] apply ALC to directed Gaussian process inference, yielding an algorithm equivalent to ours described in subsection 3.1 for a single point of interest. We note that their definition of conditional variance in Equation (5) is analogous to our (2.2), equating their conditional variance objective in Equation (8) to our (3.2) (the connection is explicitly stated in SM§4's Equation (SM.22)). They also update the precision by the blocked equations in SM§1 like our subsection SM2.3.

For inference at multiple points of interest, [21] suggests direct parallelization of the single-target algorithm over each target. They mention that the `laGP` function in their `R` package jointly considers multiple target points, but without providing details on this procedure. [57] proposes a "joint" or "path" ALC by taking the average reduction in posterior variance over target points. Instead, we generalize ALC to multiple prediction points through their posterior log determinant (5.4) and provide an explicit algorithm described in subsection 5.2. In addition, integration of the algorithm into Cholesky factorization (section 4) provides a global approximation of the Gaussian process (subsection 6.2) beyond directed local approximation.

Orthogonal matching pursuit (OMP). Our selection algorithm can be viewed as the covariance equivalent of the sparse signal recovery algorithm orthogonal matching pursuit (OMP) [59, 60]. OMP measures the approximation of a target signal by its residual after orthogonal projection onto the subspace of chosen training signals, which is efficiently calculated by maintaining a QR factorization. In contrast, our selection algorithm uses a kernel function to evaluate inner products, so orthogonalization becomes conditioning, the residual norm becomes variance, and the QR factorization becomes a Cholesky factorization. A major difference from OMP is that the computational time of conditioning dominates that of evaluating the kernel function since the feature space is relatively low-dimensional (often 2 or 3 in spatial statistics).

Sparse Cholesky factorization. Our sparse Cholesky factorization algorithm proposed in section 4 relies heavily on the KL-minimization framework of [47] and is similar to [30]. We comment that using k-nearest neighbors to select the sparsity set instead of our conditional selection algorithms essentially recovers [47] and that using the correlation objective (3.2) without conditioning on selected points recovers [30].

7.2. Conclusion. In this work, we develop an algorithm for directed Gaussian process regression which greedily selects training points that maximize mutual information with a target point, conditional on all points previously selected to avoid redundancy. We show that using conditional selection to pick the sparsity pattern of sparse approximate Cholesky factors of precision matrices significantly improves accuracy and performance in downstream tasks com-

pared to selection by nearest neighbors. Single-target conditional selection is computationally efficient and can be extended to the settings of multiple-target and partial conditioning corresponding to aggregated (or supernodal) Cholesky factorization. Finally, global selection gives a principled way of distributing nonzeros over columns of the Cholesky factor. We support these claims through extensive numerical experimentation in a variety of problems.

REFERENCES

[1] S. AMBIKASARAN AND E. DARVE, *An $\mathcal{O}(N \log N)$ fast direct solver for partial hierarchically semi-separable matrices*, Journal of Scientific Computing, 57 (2013), pp. 477–501.

[2] S. AMBIKASARAN, D. FOREMAN-MACKEY, L. GREENGARD, D. W. HOGG, AND M. O'NEIL, *Fast direct methods for Gaussian processes*, IEEE transactions on pattern analysis and machine intelligence, 38 (2015), pp. 252–265.

[3] F. R. BACH AND M. I. JORDAN, *Kernel independent component analysis*, Journal of machine learning research, 3 (2002), pp. 1–48.

[4] S. BANERJEE, A. E. GELFAND, A. O. FINLEY, AND H. SANG, *Gaussian predictive process models for large spatial data sets*, Journal of the Royal Statistical Society: Series B (Statistical Methodology), 70 (2008), pp. 825–848.

[5] S. BEHNEL, R. BRADSHAW, C. CITRO, L. DALCIN, D. S. SELJEBOTN, AND K. SMITH, *Cython: The Best of Both Worlds*, Computing in Science & Engineering, 13 (2011), pp. 31–39, https://doi.org/10.1109/MCSE.2010.118.

[6] M. BENZI AND M. TUMA, *Orderings for factorized sparse approximate inverse preconditioners*, SIAM Journal on Scientific Computing, 21 (2000), pp. 1851–1868.

[7] G. BEYLKIN, R. COIFMAN, AND V. ROKHLIN, *Fast wavelet transforms and numerical algorithms i*, Communications on pure and applied mathematics, 44 (1991), pp. 141–183.

[8] K. CHALUPKA, C. K. I. WILLIAMS, AND I. MURRAY, *A Framework for Evaluating Approximation Methods for Gaussian Process Regression*, Nov. 2012, https://doi.org/10.48550/arXiv.1205.6326, https://arxiv.org/abs/1205.6326.

[9] S. CHANDRASEKARAN, M. GU, AND T. PALS, *A fast ULV decomposition solver for hierarchically semiseparable representations*, SIAM Journal on Matrix Analysis and Applications, 28 (2006), pp. 603–622.

[10] J. CHEN, F. SCHÄFER, J. HUANG, AND M. DESBRUN, *Multiscale cholesky preconditioning for ill-conditioned problems*, ACM Transactions on Graphics (TOG), 40 (2021), pp. 1–13.

[11] Y. CHEN, E. N. EPPERLY, J. A. TROPP, AND R. J. WEBBER, *Randomly pivoted Cholesky: Practical approximation of a kernel matrix with few entry evaluations*, arXiv preprint arXiv:2207.06503, (2022).

[12] E. CLARK, T. ASKHAM, S. L. BRUNTON, AND J. N. KUTZ, *Greedy Sensor Placement with Cost Constraints*, arXiv:1805.03717 [math], (2018), https://arxiv.org/abs/1805.03717.

[13] D. A. COHN, *Neural Network Exploration Using Optimal Experiment Design*, Neural Networks, 9 (1996), pp. 1071–1083, https://doi.org/10.1016/0893-6080(95)00137-9.

[14] A. ELDERING, C. W. O'DELL, P. O. WENNBERG, D. CRISP, M. R. GUNSON, C. VIATTE, C. AVIS, A. BRAVERMAN, R. CASTANO, A. CHANG, L. CHAPSKY, C. CHENG, B. CONNOR, L. DANG, G. DORAN, B. FISHER, C. FRANKENBERG, D. FU, R. GRANAT, J. HOBBS, R. A. M. LEE, L. MANDRAKE,

J. McDuffie, C. E. Miller, V. Myers, V. Natraj, D. O'Brien, G. B. Osterman, F. Oyafuso, V. H. Payne, H. R. Pollock, I. Polonsky, C. M. Roehl, R. Rosenberg, F. Schwandner, M. Smyth, V. Tang, T. E. Taylor, C. To, D. Wunch, and J. Yoshimizu, *The Orbiting Carbon Observatory-2: First 18 months of science data products*, Atmospheric Measurement Techniques, 10 (2017), pp. 549–563, https://doi.org/10.5194/amt-10-549-2017.

[15] M. Ferronato, C. Janna, and G. Gambolati, *A novel factorized sparse approximate inverse preconditioner with supernodes*, Procedia Computer Science, 51 (2015), pp. 266–275.

[16] S. Fine and K. Scheinberg, *Efficient SVM training using low-rank kernel representations*, Journal of Machine Learning Research, 2 (2001), pp. 243–264.

[17] C. Fowlkes, S. Belongie, F. Chung, and J. Malik, *Spectral grouping using the Nystrom method*, IEEE transactions on pattern analysis and machine intelligence, 26 (2004), pp. 214–225.

[18] R. Furrer, M. G. Genton, and D. Nychka, *Covariance tapering for interpolation of large spatial datasets*, Journal of Computational and Graphical Statistics, 15 (2006), pp. 502–523.

[19] D. Gines, G. Beylkin, and J. Dunn, *LU factorization of non-standard forms and direct multiresolution solvers*, Applied and Computational Harmonic Analysis, 5 (1998), pp. 156–201.

[20] I. G. Graham, F. Y. Kuo, D. Nuyens, R. Scheichl, and I. H. Sloan, *Analysis of circulant embedding methods for sampling stationary random fields*, SIAM Journal on Numerical Analysis, 56 (2018), pp. 1871–1895.

[21] R. B. Gramacy and D. W. Apley, *Local Gaussian process approximation for large computer experiments*, Oct. 2014, https://arxiv.org/abs/1303.0383.

[22] R. B. Gramacy and B. Haaland, *Speeding up neighborhood search in local Gaussian process prediction*, Jan. 2015, https://arxiv.org/abs/1409.0074.

[23] J. Guinness, *Permutation and Grouping Methods for Sharpening Gaussian Process Approximations*, Technometrics, 60 (2018), pp. 415–429, https://doi.org/10.1080/00401706.2018.1437476, https://arxiv.org/abs/1609.05372.

[24] W. Hackbusch and S. Börm, *Data-sparse approximation by adaptive $\mathcal{H}^2$-matrices*, Computing, 69 (2002), pp. 1–35.

[25] W. Hackbusch and B. N. Khoromskij, *A sparse $\mathcal{H}$-matrix arithmetic.*, Computing, 64 (2000), pp. 21–47.

[26] C. R. Harris, K. J. Millman, S. J. van der Walt, R. Gommers, P. Virtanen, D. Cournapeau, E. Wieser, J. Taylor, S. Berg, N. J. Smith, R. Kern, M. Picus, S. Hoyer, M. H. van Kerkwijk, M. Brett, A. Haldane, J. F. del Río, M. Wiebe, P. Peterson, P. Gérard-Marchant, K. Sheppard, T. Reddy, W. Weckesser, H. Abbasi, C. Gohlke, and T. E. Oliphant, *Array programming with NumPy*, Nature, 585 (2020), pp. 357–362, https://doi.org/10.1038/s41586-020-2649-2.

[27] R. Herbrich, N. Lawrence, and M. Seeger, *Fast Sparse Gaussian Process Methods: The Informative Vector Machine*, in Advances in Neural Information Processing Systems, vol. 15, MIT Press, 2002.

[28] K. L. Ho and L. Ying, *Hierarchical interpolative factorization for elliptic operators: Integral equations*, Communications on Pure and Applied Mathematics, 7 (2016), pp. 1314–1353.

[29] J. D. Hunter, *Matplotlib: A 2D Graphics Environment*, Computing in Science & Engineering, 9 (2007), pp. 90–95, https://doi.org/10.1109/MCSE.2007.55.

[30] M. Kang and M. Katzfuss, *Correlation-based sparse inverse Cholesky factorization for fast Gaussian-process inference*, Dec. 2021, https://arxiv.org/abs/2112.14591.

[31] I. E. Kaporin, *An alternative approach to estimating the convergence rate of the CG method*, Numerical Methods and Software, Yu. A. Kuznetsov, ed., Dept. of Numerical Mathematics, USSR Academy of Sciences, Moscow, (1990), pp. 55–72.

[32] M. Katzfuss and J. Guinness, *A General Framework for Vecchia Approximations of Gaussian Processes*, Statistical Science, 36 (2021), pp. 124–141, https://doi.org/10.1214/19-STS755.

[33] M. Katzfuss and F. Schäfer, *Scalable Bayesian transport maps for high-dimensional non-Gaussian spatial fields*, Feb. 2022, https://arxiv.org/abs/2108.04211.

[34] A. Krause, A. Singh, and C. Guestrin, *Near-Optimal Sensor Placements in Gaussian Processes: Theory, Efficient Algorithms and Empirical Studies*, The Journal of Machine Learning Research, 9 (2008), pp. 235–284.

[35] Y. LeCun, L. Bottou, Y. Bengio, and P. Haffner, *Gradient-based learning applied to document*

recognition, Proceedings of the IEEE, 86 (1998), pp. 2278–2324, https://doi.org/10.1109/5.726791.

[36] S. Li, M. Gu, C. J. Wu, and J. Xia, *New efficient and robust HSS Cholesky factorization of SPD matrices*, SIAM Journal on Matrix Analysis and Applications, 33 (2012), pp. 886–904.

[37] H. Liu, Y.-S. Ong, X. Shen, and J. Cai, *When Gaussian Process Meets Big Data: A Review of Scalable GPs*, IEEE Transactions on Neural Networks and Learning Systems, 31 (2020), pp. 4405–4423, https://doi.org/10.1109/TNNLS.2019.2957109.

[38] Y. Marzouk, T. Moselhy, M. Parno, and A. Spantini, *An introduction to sampling via measure transport*, arXiv:1602.05023 [math, stat], (2016), pp. 1–41, https://doi.org/10.1007/978-3-319-11259-6_23-1, https://arxiv.org/abs/1602.05023.

[39] M. Mutný and A. Krause, *Experimental Design for Linear Functionals in Reproducing Kernel Hilbert Spaces*, May 2022, https://arxiv.org/abs/2205.13627.

[40] H. Owhadi and C. Scovel, *Operator-Adapted Wavelets, Fast Solvers, and Numerical Homogenization: From a Game Theoretic Approach to Numerical Approximation and Algorithm Design*, Cambridge Monographs on Applied and Computational Mathematics, Cambridge University Press, Cambridge, 2019, https://doi.org/10.1017/9781108594967.

[41] F. Pedregosa, G. Varoquaux, A. Gramfort, V. Michel, B. Thirion, O. Grisel, M. Blondel, P. Prettenhofer, R. Weiss, V. Dubourg, J. Vanderplas, A. Passos, D. Cournapeau, M. Brucher, M. Perrot, and É. Duchesnay, *Scikit-learn: Machine Learning in Python*, Journal of Machine Learning Research, 12 (2011), pp. 2825–2830.

[42] J. Quiñonero-Candela and C. E. Rasmussen, *A Unifying View of Sparse Approximate Gaussian Process Regression*, Journal of Machine Learning Research, 6 (2005), pp. 1939–1959.

[43] A. Rahimi and B. Recht, *Random features for large-scale kernel machines*, Advances in neural information processing systems, 20 (2007).

[44] C. E. Rasmussen and C. K. I. Williams, *Gaussian Processes for Machine Learning*, Adaptive Computation and Machine Learning, MIT Press, Cambridge, Mass, 2006.

[45] H. Rue and L. Held, *Gaussian Markov Random Fields: Theory and Applications*, Chapman and Hall/CRC, New York, Feb. 2005, https://doi.org/10.1201/9780203492024.

[46] H. Sang and J. Z. Huang, *A full scale approximation of covariance functions for large spatial data sets*, Journal of the Royal Statistical Society: Series B (Statistical Methodology), 74 (2012), pp. 111–132.

[47] F. Schäfer, M. Katzfuss, and H. Owhadi, *Sparse Cholesky factorization by Kullback-Leibler minimization*, arXiv:2004.14455 [cs, math, stat], (2021), https://arxiv.org/abs/2004.14455.

[48] F. Schäfer, T. J. Sullivan, and H. Owhadi, *Compression, inversion, and approximate PCA of dense kernel matrices at near-linear computational complexity*, arXiv:1706.02205 [cs, math], (2020), https://arxiv.org/abs/1706.02205.

[49] A. Schwaighofer and V. Tresp, *Transductive and inductive methods for approximate Gaussian process regression*, Advances in neural information processing systems, 15 (2002).

[50] M. Seeger and C. K. I. Williams, *Fast Forward Selection to Speed Up Sparse Gaussian Process Regression*, in In Workshop on AI and Statistics 9, 2003.

[51] A. Smola and P. Bartlett, *Sparse Greedy Gaussian Process Regression*, in Advances in Neural Information Processing Systems, vol. 13, MIT Press, 2000.

[52] A. Spantini, D. Bigoni, and Y. Marzouk, *Inference via low-dimensional couplings*, July 2018, https://doi.org/10.48550/arXiv.1703.06131, https://arxiv.org/abs/1703.06131.

[53] M. L. Stein, *Fast and exact simulation of fractional Brownian surfaces*, Journal of Computational and Graphical Statistics, 11 (2002), pp. 587–599.

[54] M. L. Stein, *The screening effect in Kriging*, The Annals of Statistics, 30 (2002), pp. 298–323, https://doi.org/10.1214/aos/1015362194.

[55] M. L. Stein, *2010 Rietz lecture: When does the screening effect hold?*, The Annals of Statistics, 39 (2011), pp. 2795–2819, https://doi.org/10.1214/11-AOS909.

[56] M. L. Stein, Z. Chi, and L. J. Welty, *Approximating likelihoods for large spatial data sets*, Journal of the Royal Statistical Society: Series B (Statistical Methodology), 66 (2004), pp. 275–296.

[57] F. Sun, R. B. Gramacy, B. Haaland, E. Lawrence, and A. Walker, *Emulating satellite drag from large simulation experiments*, June 2019, https://doi.org/10.48550/arXiv.1712.00182, https://arxiv.org/abs/1712.00182.

[58] W. Sweldens, *The lifting scheme: A custom-design construction of biorthogonal wavelets*, Applied and

computational harmonic analysis, 3 (1996), pp. 186–200.

[59] J. A. TROPP AND A. C. GILBERT, *Signal Recovery From Random Measurements Via Orthogonal Matching Pursuit*, IEEE Transactions on Information Theory, 53 (2007), pp. 4655–4666, https://doi.org/10.1109/TIT.2007.909108.

[60] J. A. TROPP, A. C. GILBERT, AND M. J. STRAUSS, *Algorithms for simultaneous sparse approximation. Part I: Greedy pursuit*, Signal Processing, 86 (2006), pp. 572–588, https://doi.org/10.1016/j.sigpro.2005.05.030.

[61] A. V. VECCHIA, *Estimation and Model Identification for Continuous Spatial Processes*, Journal of the Royal Statistical Society: Series B (Methodological), 50 (1988), pp. 297–312, https://doi.org/10.1111/j.2517-6161.1988.tb01729.x.

[62] S. VIJAYAKUMAR AND S. SCHAAL, *Locally weighted projection regression: An O (n) algorithm for incremental real time learning in high dimensional space*, Proceedings of the Seventeenth International Conference on Machine Learning (ICML 2000), (2000), pp. 1079–1086.

[63] P. VIRTANEN, R. GOMMERS, T. E. OLIPHANT, M. HABERLAND, T. REDDY, D. COURNAPEAU, E. BUROVSKI, P. PETERSON, W. WECKESSER, J. BRIGHT, S. J. VAN DER WALT, M. BRETT, J. WILSON, K. J. MILLMAN, N. MAYOROV, A. R. J. NELSON, E. JONES, R. KERN, E. LARSON, C. J. CAREY, İ. POLAT, Y. FENG, E. W. MOORE, J. VANDERPLAS, D. LAXALDE, J. PERKTOLD, R. CIMRMAN, I. HENRIKSEN, E. A. QUINTERO, C. R. HARRIS, A. M. ARCHIBALD, A. H. RIBEIRO, F. PEDREGOSA, AND P. VAN MULBREGT, *SciPy 1.0: Fundamental algorithms for scientific computing in Python*, Nature Methods, 17 (2020), pp. 261–272, https://doi.org/10.1038/s41592-019-0686-2.

[64] T. WADA, Y. MATSUMURA, S. MAEDA, AND H. SHIBUYA, *Gaussian Process Regression with Dynamic Active Set and Its Application to Anomaly Detection*, in Proceedings of the International Conference on Data Science (ICDATA), 2013, p. 7.

[65] C. WILLIAMS AND M. SEEGER, *Using the Nyström method to speed up kernel machines*, Advances in neural information processing systems, 13 (2000).

[66] J. XIA, S. CHANDRASEKARAN, M. GU, AND X. S. LI, *Fast algorithms for hierarchically semiseparable matrices*, Numerical Linear Algebra with Applications, 17 (2010), pp. 953–976.

[67] A. Y. YEREMIN, L. Y. KOLOTILINA, AND A. A. NIKISHIN, *Factorized sparse approximate inverse preconditionings. III. Iterative construction of preconditioners*, Journal of Mathematical Sciences, 101 (2000), pp. 3237–3254, https://doi.org/10.1007/BF02672769.

Appendix A. Derivations in KL-minimization.

A.1. KL divergence of optimal factor.

Proof of Equation (2.12). From the closed-form expression for the KL divergence in (2.10) and defining $\Delta \coloneqq 2\mathbb{D}_{\mathrm{KL}}\big(\mathcal{N}(\mathbf{0}, \Theta) \,\big\|\, \mathcal{N}(\mathbf{0}, (LL^\top)^{-1})\big)$ for brevity of notation,

$$(A.1) \qquad \Delta = \mathrm{trace}(LL^\top \Theta) - \mathrm{logdet}(LL^\top) - \mathrm{logdet}(\Theta) - N.$$

Focusing on the term $\mathrm{trace}(LL^\top \Theta) = \mathrm{trace}(L^\top \Theta L)$ by the cyclic property of trace and using the sparsity of L by plugging in the definition (2.11) for each column $L_{s_i,i}$,

$$(A.2) \qquad \mathrm{trace}(L^\top \Theta L) = \sum_{i=1}^{N} L_{s_i,i}^\top \Theta_{s_i,s_i} L_{s_i,i}$$

$$(A.3) \qquad = \sum_{i=1}^{N} \left(\frac{(\Theta_{s_i,s_i}^{-1} \boldsymbol{e}_1)^\top}{\sqrt{\boldsymbol{e}_1^\top \Theta_{s_i,s_i}^{-1} \boldsymbol{e}_1}}\right) \Theta_{s_i,s_i} \left(\frac{\Theta_{s_i,s_i}^{-1} \boldsymbol{e}_1}{\sqrt{\boldsymbol{e}_1^\top \Theta_{s_i,s_i}^{-1} \boldsymbol{e}_1}}\right)$$

$$(A.4) \qquad = \sum_{i=1}^{N} \frac{\boldsymbol{e}_1^\top \Theta_{s_i,s_i}^{-1} \Theta_{s_i,s_i} \Theta_{s_i,s_i}^{-1} \boldsymbol{e}_1}{\boldsymbol{e}_1^\top \Theta_{s_i,s_i}^{-1} \boldsymbol{e}_1} = \sum_{i=1}^{N} 1 = N,$$

exactly the constraint $\mathrm{diag}(L^\top \Theta L) = 1$ from subsection 2.1. Substituting back into (A.1),

$$(A.5) \qquad \Delta = -\mathrm{logdet}(LL^\top) - \mathrm{logdet}(\Theta).$$

Computing the log determinant of a triangular matrix as the sum of the log of its diagonal entries and plugging in the definition (2.11) for the diagonal entries,

$$(A.6) \qquad = -\sum_{i=1}^{N} \left[\log(\boldsymbol{e}_1^\top \Theta_{s_i,s_i}^{-1} \boldsymbol{e}_1)\right] - \mathrm{logdet}(\Theta)$$

$$(A.7) \qquad = \sum_{i=1}^{N} \left[\log\left((\boldsymbol{e}_1^\top \Theta_{s_i,s_i}^{-1} \boldsymbol{e}_1)^{-1}\right)\right] - \mathrm{logdet}(\Theta).$$

Now we use that conditioning in covariance is marginalization in precision,

$$(A.8) \qquad \Theta_{1,1|2} = \big(\Theta^{-1}\big)_{1,1}^{-1} \qquad \text{for } \Theta = \begin{pmatrix} \Theta_{1,1} & \Theta_{1,2} \\ \Theta_{2,1} & \Theta_{2,2} \end{pmatrix}.$$

Transforming the marginalization $(\boldsymbol{e}_1^\top \Theta_{s_i,s_i}^{-1} \boldsymbol{e}_1)^{-1} = \big(\Theta_{s_i,s_i}^{-1}\big)_{1,1}^{-1} = \Theta_{i,i|s_i \setminus \{i\}}$ by (A.8),

$$(A.9) \qquad \Delta = \sum_{i=1}^{N} \left[\log\left(\Theta_{i,i|s_i \setminus \{i\}}\right)\right] - \mathrm{logdet}(\Theta).$$

Now we use the chain rule of log determinants, using the same blocking as (A.8),

$$(A.10) \qquad \mathrm{logdet}(\Theta) = \mathrm{logdet}(\Theta_{1,1}) + \mathrm{logdet}(\Theta_{2,2|1}).$$

Repeatedly expanding the log determinant by (A.10), working from back to front,

$$(A.11) \qquad \Delta = \sum_{i=1}^{N} \log\left(\Theta_{i,i|s_i \setminus \{i\}}\right) - \sum_{i=1}^{N} \log\left(\Theta_{i,i|i+1:}\right)$$

Figure 17. *Illustration of the Cholesky factorization of a partially conditioned covariance matrix. Here* grey *denotes fully unconditional,* blue *denotes fully conditional, and the* mixed color *denotes interaction between the two. Surprisingly, such a matrix factors into a "pure" Cholesky factor by "gluing" the prefix of the fully unconditional factor with the suffix of the fully conditional factor.*

802 (A.12)
$$= \sum_{i=1}^{N} \left[\log \left(\Theta_{i,i|s_i \setminus \{i\}} \right) - \log \left(\Theta_{i,i|i+1:} \right) \right]. \qquad \blacksquare$$

803 ## A.2. Aggregated KL divergence.

804 *Proof of Equation* (5.1). The KL divergence (2.12) restricted to the group $\tilde{i}$ is

805 (A.13)
$$\sum_{i \in \tilde{i}} \log(\Theta_{i|s_i \setminus \{i\}}) = \log(\Theta_{i_1|\tilde{s}}) + \log(\Theta_{i_2|\tilde{s} \cup \{i_1\}}) + \cdots + \log(\Theta_{i_m|\tilde{s} \cup \tilde{i}})$$

806 where we write $\Theta_j := \Theta_{j,j}$. Combining the first two terms by the chain rule (A.10),

807 (A.14)
$$= \text{logdet}(\Theta_{\{i_1,i_2\}|\tilde{s}}) + \log(\Theta_{i_3|\tilde{s} \cup \{i_1,i_2\}}) + \cdots + \log(\Theta_{i_m|\tilde{s} \cup \tilde{i}}).$$

808 Proceeding by induction, we are able to reduce the entire sum to the single term

809 (A.15)
$$= \text{logdet}(\Theta_{\tilde{i},\tilde{i}|\tilde{s}}). \qquad \blacksquare$$

810 ## A.3. Partial KL divergence.

811 *Proof of Equation* (5.3). The original variables $\boldsymbol{y}$ have joint density multivariate Gaussian,
812 $\boldsymbol{y} \sim \mathcal{N}(\boldsymbol{0}, \Theta)$ for some covariance matrix Θ so the fully conditional variables $\boldsymbol{y}_{|k}$ have posterior
813 distribution from (2.1) and (2.2), $\boldsymbol{y}_{|k} \sim \mathcal{N}(\boldsymbol{\mu}, \Theta_{:,:|k})$ for some posterior mean $\boldsymbol{\mu}$. The covariance
814 of unconditioned y_i and y_j is $\Theta_{i,j}$ by definition; similarly, the covariance of conditioned $y_{i|k}$
815 and $y_{j|k}$ is $\Theta_{i,j|k}$. We must compute the covariance between unconditioned y_i and conditioned
816 $y_{j|k}$. Let $L = \text{chol}(\Theta)$ and $L' = \text{chol}(\Theta_{:,:|k})$ so that $\boldsymbol{y} = L\boldsymbol{z}$ for $\boldsymbol{z} \sim \mathcal{N}(\boldsymbol{0}, \text{Id})$ and $\boldsymbol{y}_{|k} = L'\boldsymbol{z} + \boldsymbol{\mu}$.
817 By the definition of covariance,

818 (A.16)
$$\mathbb{C}\text{ov}[y_i, y_{j|k}] = \mathbb{E}[(y_i - \mathbb{E}[y_i])(y_{j|k} - \mathbb{E}[y_{j|k}])] = \mathbb{E}[(L_i \boldsymbol{z})(L'_j \boldsymbol{z} + \mu_j - \mu_j)]$$

819 (A.17)
$$= \mathbb{E}[(L_{i,1} z_1 + \cdots + L_{i,m} z_m)(L'_{j,1} z_1 + \cdots + L'_{j,m} z_m)].$$

820 For $i \neq j$, $\mathbb{E}[z_i z_j] = \mathbb{E}[z_i]\mathbb{E}[z_j] = 0$ since z_i is independent of z_j and has mean 0,

821 (A.18)
$$= L_{i,1} L'_{j,1} \mathbb{E}[z_1^2] + \cdots + L_{i,m} L'_{j,m} \mathbb{E}[z_m^2].$$

822 For any i, $\mathbb{E}[z_i^2] = \mathbb{V}\text{ar}[z_i] + \mathbb{E}[z_i]^2 = 1 + 0 = 1$,

823 (A.19)
$$= L_{i,1} L'_{j,1} + \cdots + L_{i,m} L'_{j,m} = L_i^\top L'_j.$$

824 Thus, the new covariance matrix factors into two Cholesky factors "glued" together,

825 (A.20)
$$\mathbb{C}\mathrm{ov}[\boldsymbol{y}_{\|k}] = \begin{pmatrix} L_{:p}L_{:p}^\top & L_{:p}L'^\top_{p+1:} \\ L'_{p+1:}L_{:p}^\top & L'_{p+1:}L'^\top_{p+1:} \end{pmatrix} = \begin{pmatrix} L_{:p} \\ L'_{p+1:} \end{pmatrix} \begin{pmatrix} L_{:p} \\ L'_{p+1:} \end{pmatrix}^\top$$

826 which is illustrated in Figure 17. Armed with this representation, we equate the log determi-
827 nant of $\Theta_{\tilde{i},\tilde{i}\|k} := \mathbb{C}\mathrm{ov}[\boldsymbol{y}_{\|k}]$ to the KL divergence in (2.12). Recalling that the determinant of
828 a triangular matrix is the product of its diagonal entries,

829
$$\frac{1}{2}\mathrm{logdet}(\Theta_{\tilde{i},\tilde{i}\|k}) = \underbrace{\log(L_{1,1}) + \cdots + \log(L_{p,p})}_{\text{the same}} + \underbrace{\log(L'_{p+1,p+1}) + \cdots + \log(L'_{m,m})}_{\text{conditioned}}.$$

830 Comparing to the KL divergence (2.12) and recalling that k is added to s_i if $i > p$,

831 (A.21)
$$\sum_{i=1}^m \log\left(\Theta_{i,i|s_i\setminus\{i\}}\right) = \underbrace{\log\left(\Theta_{1,1|s_1\setminus\{1\}}\right) + \cdots + \log\left(\Theta_{p,p|s_p\setminus\{p\}}\right)}_{\text{the same}} +$$

832
$$\underbrace{\log\left(\Theta_{p+1,p+1|s_{p+1}\setminus\{p+1\}}\right) + \cdots + \log\left(\Theta_{m,m|s_m\setminus\{m\}}\right)}_{\text{conditioned}}.$$

Since $L_{i,i}$ (and $L'_{i,i}$) is the square root of the posterior variance of the ith variable from the
833 statistical perspective in (SM2.6), we have $2\log(L_{i,i}) = \log(\Theta_{i,i|s_i\setminus\{i\}})$ and so

834 (A.22)
$$\mathrm{logdet}(\Theta_{\tilde{i},\tilde{i}\|k}) = \sum_{i=1}^m \log\left(\Theta_{i,i|s_i\setminus\{i\}}\right). \qquad \blacksquare$$